Supporting Online Information for
Optical pKa Control in a Bifunctional Iridium Complex

Ivan Demianets, Jonathan R. Hunt, Jahan M. Dawlaty*, and Travis J. Williams*

Donald P. and Katherine B. Loker Hydrocarbon Institute and Department of Chemistry, University of Southern California, Los Angeles, California, 90089-1661, United States

dawlaty@usc.edu, travisw@usc.edu

Contents

S1. Materials and Methods

All air and moisture sensitive procedures were carried out in a Vacuum Atmospheres glove box under nitrogen or using standard Schlenk techniques. NMR solvents were purchased from Cambridge Isotopes Laboratories. Dichloromethane-d_2 was dried by stirring over CaH_2 for 1 day followed by vapor transfer into a dry flask; chloroform-d_3 was used as received. Hexanes, ethyl ether, dichloromethane and tetrahydrofuran solvents were purchased from VWR and dried in a J. C. Meyer solvent purification system with alumina/copper(II) oxide columns. Methanol, ethanol, isopropanol, 2,2,2-trifluoethanol and hexafluoroisopropanol were dried by stirring over CaH_2 (5% w/v) overnight, followed by vapor transfer into a dry flask. 2,2,2-Trifluoethanol and hexafluoroisopropanol were stirred over Na_2CO_3 (10% w/v) over 1 hour then separated by a vapor transfer step. Chloro(1,5-cyclooctadiene)iridium(I) dimer (Strem), sodium trifluoromethanesulfonate (Sigma-Aldrich), sodium hydride (Sigma-Aldrich) were purged with nitrogen and stored under nitrogen atmosphere. Starting materials as well as reagents were purchased from the following list of vendors: Sigma-Aldrich, Strem Chemicals, TCI, VWR, Oakwood Chemicals, Chem Impex, Alpha Aesar, Combi Blocks, Acros and Ark Pharm. Known compounds were synthesized using literature procedures directly or with slight modification; new compounds syntheses are described in section S2. Synthesis Procedures and Characterization Data.

NMR spectra were recorded on a Varian 400MR, VNMRS-500, or VNMRS-600 spectrometer and processed using MestreNova. Chemical shifts are reported in units of ppm and referenced to the residual ^{1}H or ^{13}C solvent peak and line-listed according to (s) singlet, (bs) broad singlet, (d) doublet, (t) triplet, (dd) double doublet, etc. ^{13}C spectra are delimited by carbon peaks, not carbon count. Air-sensitive NMR spectra were taken in J-Young tubes (Wilmad or Norell) with Teflon valve plugs. Mass mass spectra were obtained on Bruker Autoflex Speed MALDI MS spectrometer using the evaporated drop method on a coated plate or Agilent Q-Tof tandem mass spectrometer. The matrices used for MALDI are 2,5-dihydroxybenzoic acid or anthracene. X-ray crystallography data were obtained on a Bruker APEX DUO single-crystal diffractometer equipped with an APEX2 CCD detector, Mo fine-focus and Cu micro-focus X-ray sources. IR spectra were obtained using Jasco FT/IR-4600 FT-IR Spectrometer. Spectral data was obtained on Perkin-Elmer UV-Vis-NIR and Horiba Fluorimeter. Concentration of the complexes solutions for absorption and emission studies was $1.4 \cdot 10^{-4}$ M and concentration of quinoline was $2.5 \cdot 10^{-5}$ M. Q-Tof samples were treated with activated carbon (10% w/v) and stirred for 10 minutes, then filtrated through a Teflon syringe filter.

S2. Synthesis Procedures and Characterization Data

*Complexes **1**, **2**, and related compounds.*

8-Bromoquinoline (4).

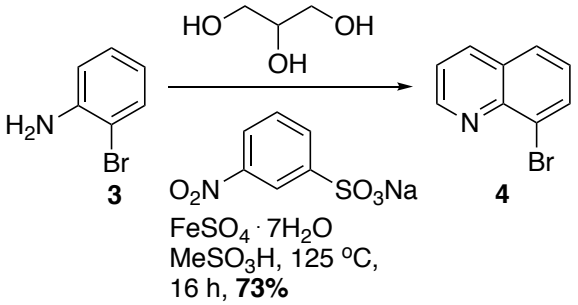

Following a modified procedure by Douglas et al.,[1] 8-bromoquinoline was synthesized by adding 15 mL of methane sulfonic acid to a 100 mL 3-neck round bottom flask with magnetic stir bar inside. The flask was heated to 125 °C and 2-bromoaniline (4.0 g, 0.0233 mol, 1 equiv.) was added portionwise over the course of 10 minutes, followed by sodium 3-nitrobenzenesulfonate (3.3 g, 0.0147 mol, 0.63 equiv.) and $FeSO_4$•$7H_2O$ (0.2 g, 0.719 mmol, 0.03 equiv.). Glycerol (5.1 mL, 0.0698 mol, 3 equiv.) was added in three portions (3 × 1.7 mL) using an addition funnel in 2 hour intervals. After the addition of the last portion of glycerol, the flask was left for 12 hours at 125 °C. The flask was cooled down to room temperature and the brown contents were transferred to a 500 mL beaker with the help of 100 mL of water. The content of the beaker was placed in an ice bath and treated with 50% w/v NaOH until pH reached 14. The heterogeneous mixture was extracted three times with diethyl ether (3 × 50 mL). Layer separation appeared to be slow, in some cases over an hour. Combined organic layers where washed with brine, dried with $MgSO_4$, filtered through the Celite pad and evaporated. The obtained brown oil was distilled under vacuum yielding a high viscosity yellow oil (3.5 g, 0.0168 mol, 73%). The obtained product matched reported NMR spectra for 8-bromoquinoline.

^{1}H NMR (600 MHz, Chloroform-*d*) δ 9.06 (dd, *J* = 4.2, 1.7 Hz, 1H), 8.18 (dd, *J* = 8.2, 1.7 Hz, 1H), 8.07 (dd, *J* = 7.5, 1.3 Hz, 1H), 7.80 (dd, *J* = 8.2, 1.3 Hz, 1H), 7.48 (dd, *J* = 8.2, 4.2 Hz, 1H), 7.41 (t, *J* = 7.8 Hz, 1H).

^{13}C NMR (101 MHz, Chloroform-*d*) δ 151.28, 151.26, 145.31, 136.62, 133.20, 129.58, 127.80, 127.76, 127.04, 127.02, 126.98, 124.80, 121.97, 121.96, 121.94, 121.89.

Methyl quinoline-8-carboxylate (5).

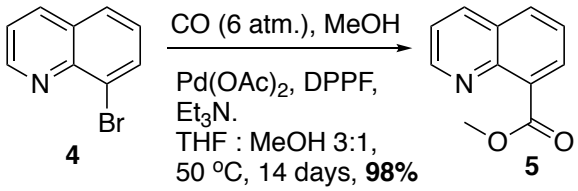

8-Bromoquinoline (2.77 g, 13.3 mmol, 1 equiv) was transferred to a 125 mL high pressure Parr apparatus, followed by the addition of 1,1'-ferrocenediyl-bis(diphenylphosphine) (DPPF) (0.59 g, 1.06 mmol, 8 mol %), palladium(II) acetate (0.12g, 0.53 mmol, 4 mol %) and Et_3N (5.56 mL, 39.9 mmol, 3 equiv.). 9 mL of dry methanol and 3 mL of dry THF were added after. The Parr apparatus was charged with 6 atm. of carbon monoxide and maintained at 50 °C for 7 days. After allowing the apparatus to cool down to room temperature, gas from inside of it was released completely and then it was repeatedly charged with 6 atm. of carbon monoxide and maintained again at 50 °C for 7 days. The Parr apparatus was cooled to room temperature, the gas was released, and the reaction mixture was filtrated through the silica pad and later evaporated. The resulting brown oil underwent purification on a flash purification system (Hex, EtOAc solvents gradient) and the collected combined fractions were evaporated. Yellow oil (2.43g, 13.0 mmol, 98%) was acquired and analyzed by NMR. The results matched previously reported spectra for the assigned compound.

^{1}H NMR (400 MHz, Chloroform-*d*) δ 9.06 (dt, *J* = 4.2, 1.6 Hz, 1H), 8.20 (dt, *J* = 8.3, 1.5 Hz, 1H), 8.04 (dt, *J* = 7.2, 1.4 Hz, 1H), 7.96 (dt, *J* = 8.2, 1.4 Hz, 1H), 7.58 (ddd, *J* = 8.2, 7.2, 1.1 Hz, 1H), 7.47 (ddd, *J* = 8.3, 4.2, 1.2 Hz, 1H), 4.12 – 4.00 (m, 3H).

^{13}C NMR (101 MHz, Chloroform-*d*) δ 167.94, 151.00, 145.02, 135.94, 131.32, 130.99, 129.88, 127.96, 125.22, 121.29, 52.24.

8-(Hydroxydi(pyridin-2-yl)methyl)quinoline (6).

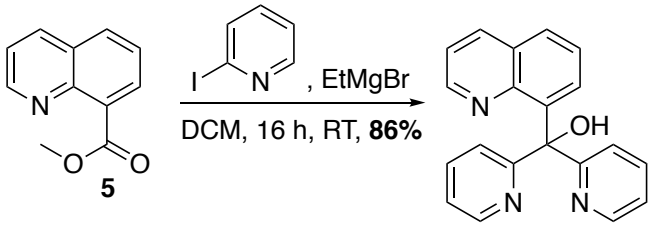

2-Iodopyridine (0.5 mL, 3.84 mmol, 2.4 equiv.) was added to a previously flame dried 250 mL flask with a magnetic stir bar inside of the glove box, followed by the addition of 60 mL of dry DCM. The flask was sealed with a rubber stopper and taken outside of the glove box, later to be connected to the nitrogen line. 3M solution of EtMgBr in diethyl ester (1.3 mL, 3.84 mmol, 2.4 equiv.) in a syringe with a needle was added dropwise to the stirring DCM solution of 2-iodopyridine through the rubber stopper and left for 45 minutes. Solution of methyl quinoline-8-carboxylate (300 mg, 1.60 mmol, 1 equiv.) in 5 mL of dry DCM was added dropwise in the same way and left for 16 hours. Reaction solution was washed with saturated $NaHCO_3$ solution of 30 mL, which was then extracted twice with DCM (2 × 15 mL). Combined DCM fractions where dried over $MgSO_4$, treated with activated charcoal, filtered through Celite pad and evaporated. The resulting yellow oil was recrystallized from boiling diethyl ether resulting in white crystals (431 mg, 1.38 mmol, 86%) that were further analyzed by NMR and proved to be spectroscopically pure.

^{1}H NMR (400 MHz, Chloroform-d) δ 8.96 (s, 1H), 8.67 – 8.62 (m, 1H), 8.53 (ddt, J = 4.8, 2.0, 1.0 Hz, 2H), 8.22 – 8.15 (m, 1H), 7.77 – 7.65 (m, 5H), 7.44 (ddd, J = 8.2, 7.2, 0.9 Hz, 1H), 7.35 (ddd, J = 8.3, 4.3, 0.9 Hz, 1H), 7.28 (t, J = 1.2 Hz, 1H), 7.16 – 7.11 (m, 2H).

^{13}C NMR (101 MHz, Chloroform-d) δ 164.83, 148.20, 148.15, 147.74, 147.69, 146.69, 141.75, 137.27, 136.25, 136.21, 130.43, 129.04, 127.70, 126.01, 122.52, 122.49, 122.47, 121.72, 121.67, 120.50, 120.43, 84.10.

FTIR ν 3087.48, 3047.94, 3006.96, 2360.93, 2338.75, 2080.82, 2022.96, 1992.59, 1956.43, 1905.33, 1853.74, 1786.24, 1735.14, 1611.23, 1585.2, 1565.43, 1496.01, 1462.74, 1427.07, 1365.35, 1311.84, 1287.25, 1242.9, 1211.08, 1164.79, 1147.44, 1103.57, 1042.82, 988.821, 937.717, 920.843, 894.809, 826.348, 779.101, 762.709, 727.514, 700.516, 676.41, 635.912, 615.663, 540.453, 496.098, 462.832

MS (MALDI) calculated for $C_{20}H_{15}N_3O$ 313.12, found 314.03.

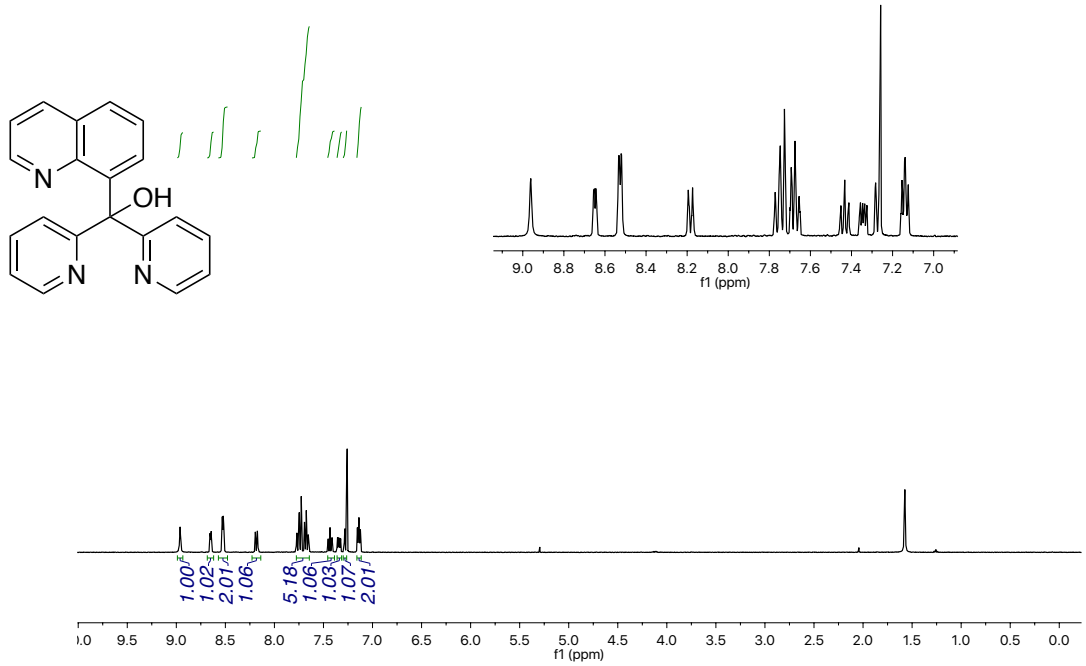

Figure S1. ^{1}H NMR spectrum of ligand **6** at 25 °C in $CDCl_3$.

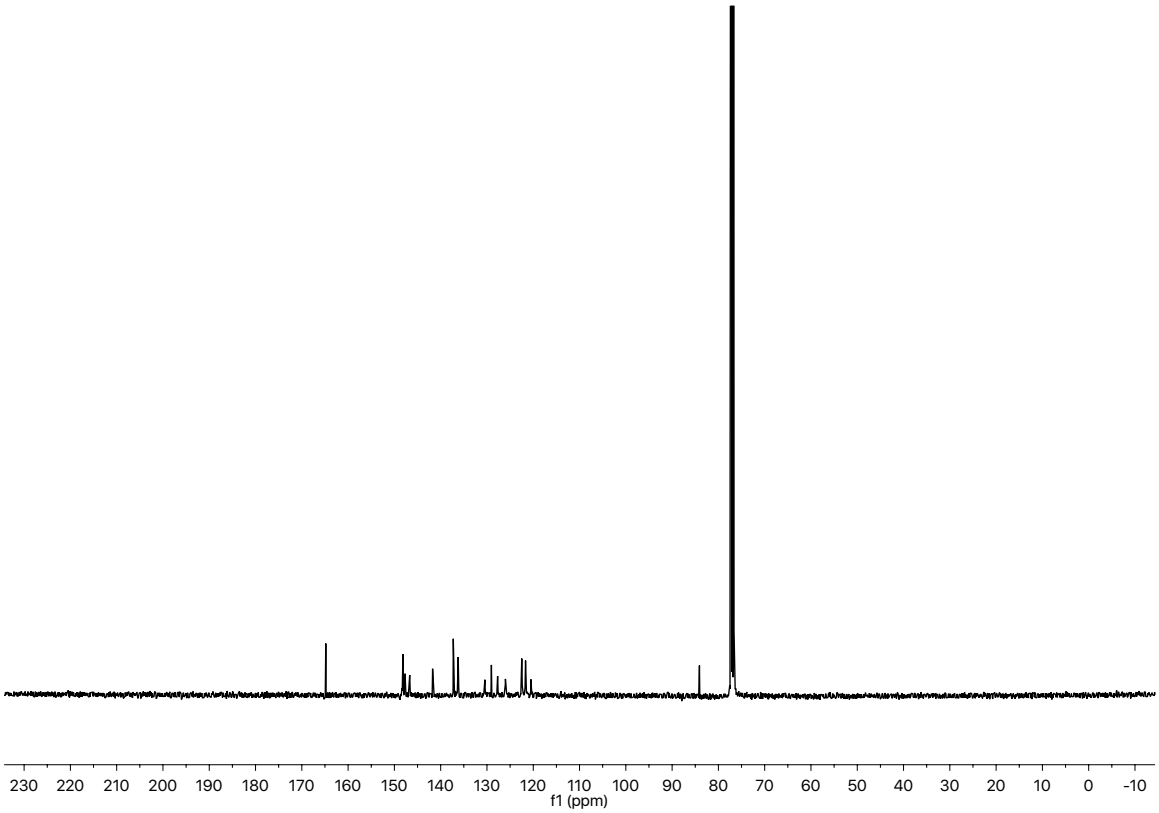

Figure S2. ^{13}C NMR spectrum of ligand **6** at 25 °C in $CDCl_3$.

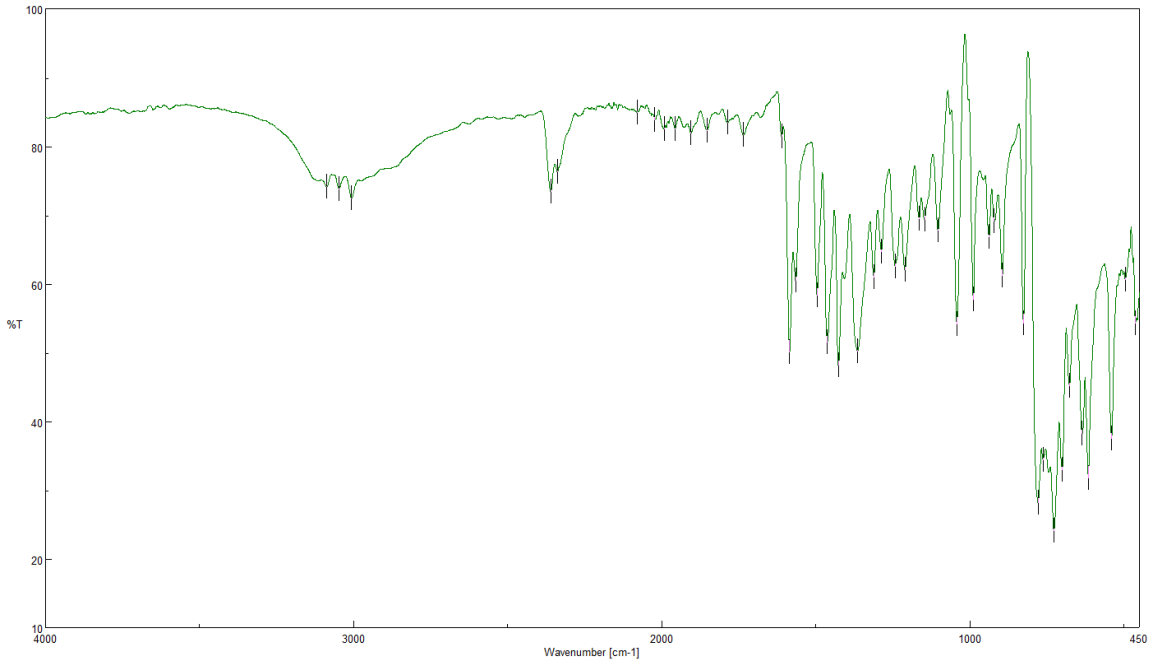

Figure S3. IR spectrum of ligand **6**.

8-(Methoxydi(pyridin-2-yl)methyl)quinoline (7).

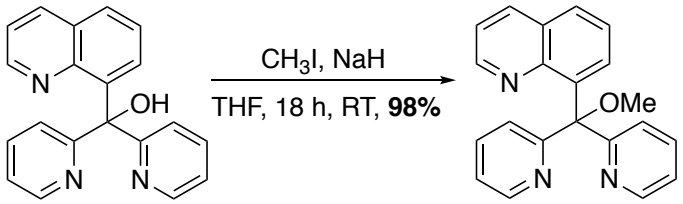

In the glovebox under nitrogen, 8-(hydroxydi(pyridin-2-yl)methyl)quinoline **6** (50 mg, 0.16 mmol, 1 equiv) and sodium hydride (15 mg, 0.64 mmol, 4 equiv) were mixed together in an 8 dram vial with a previously placed magnetic stir bar. Iodomethane (40 μL, 0.64 mmol, 4 equiv.) was added to 3 mL of THF and this solution was transferred to the vial. The stirring solution was left for 18 hours and then slowly quenched with 20 mL of saturated $NaHCO_3$ outside of the glove box. The resulting solution was extracted with DCM (3 × 15 mL) and fractions were combined, dried over $MgSO_4$, and concentrated. The resulting grey powder (52 mg, 0.16 mmol, 98%) appeared to be spectroscopically pure under NMR.

^{1}H NMR (400 MHz, Chloroform-d) δ 8.54 – 8.49 (m, 2H), 8.49 – 8.46 (m, 1H), 8.12 (dd, J = 7.4, 1.4 Hz, 1H), 8.09 – 8.02 (m, 1H), 7.83 (dt, J = 8.1, 1.1 Hz, 2H), 7.79 (dd, J = 8.2, 1.4 Hz, 1H), 7.62 – 7.53 (m, 3H), 7.22 – 7.16 (m, 1H), 7.06 (dddd, J = 7.5, 4.8, 1.2, 0.5 Hz, 2H), 3.26 (d, J = 0.6 Hz, 3H).

^{13}C NMR (101 MHz, Chloroform-d) δ 162.53, 147.99, 147.90, 139.87, 135.90, 131.03, 128.83, 121.17, 120.18, 87.44, 52.91.

FTIR ν 3051.8, 3003.11, 2935.13, 2831.47, 1585.68, 1568.81, 1496.01, 1462.74, 1429.48, 1382.23, 1309.91, 1240, 1198.06, 1156.12, 1132.97, 1105.01, 1080.91, 1047.64, 993.643, 965.198, 946.395, 910.236, 887.577, 828.759, 790.671, 764.155, 744.388, 709.194, 673.035, 635.43, 616.627, 582.397, 558.773, 533.703, 503.33, 486.456, 458.975.

MS (MALDI) calculated for $C_{21}H_{17}N_3O$ 327.14, found 327.91.

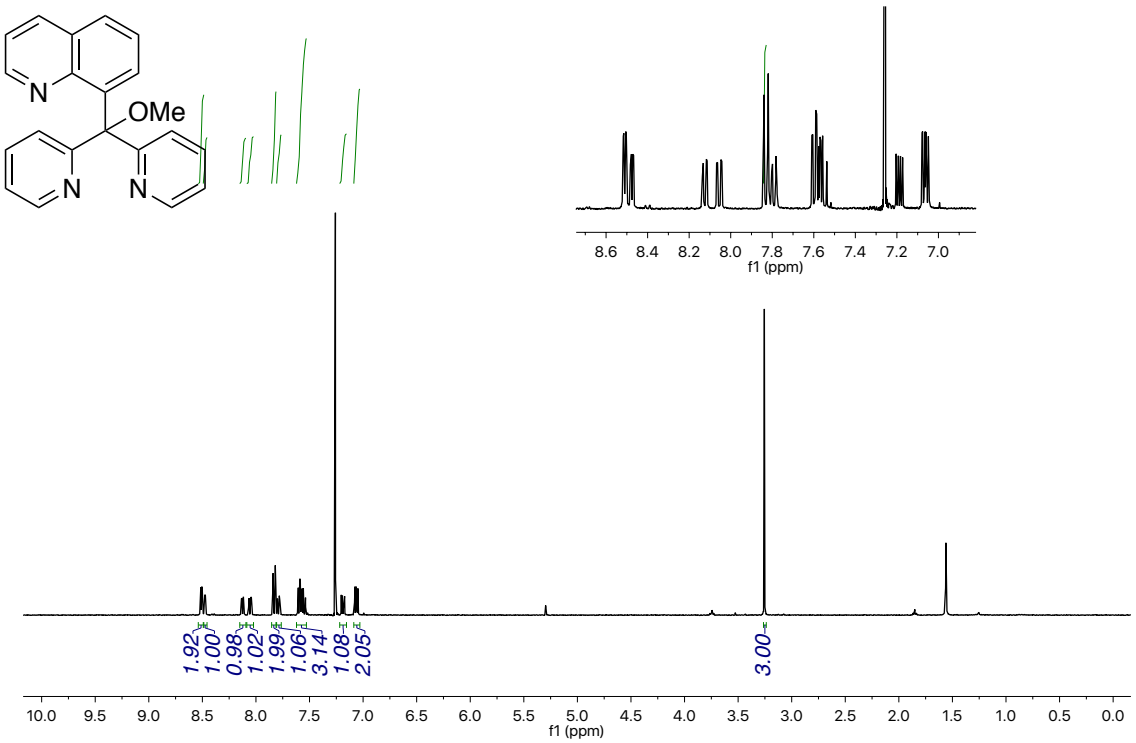

Figure S4. ^{1}H NMR spectrum of ligand **7** at 25 °C in $CDCl_3$.

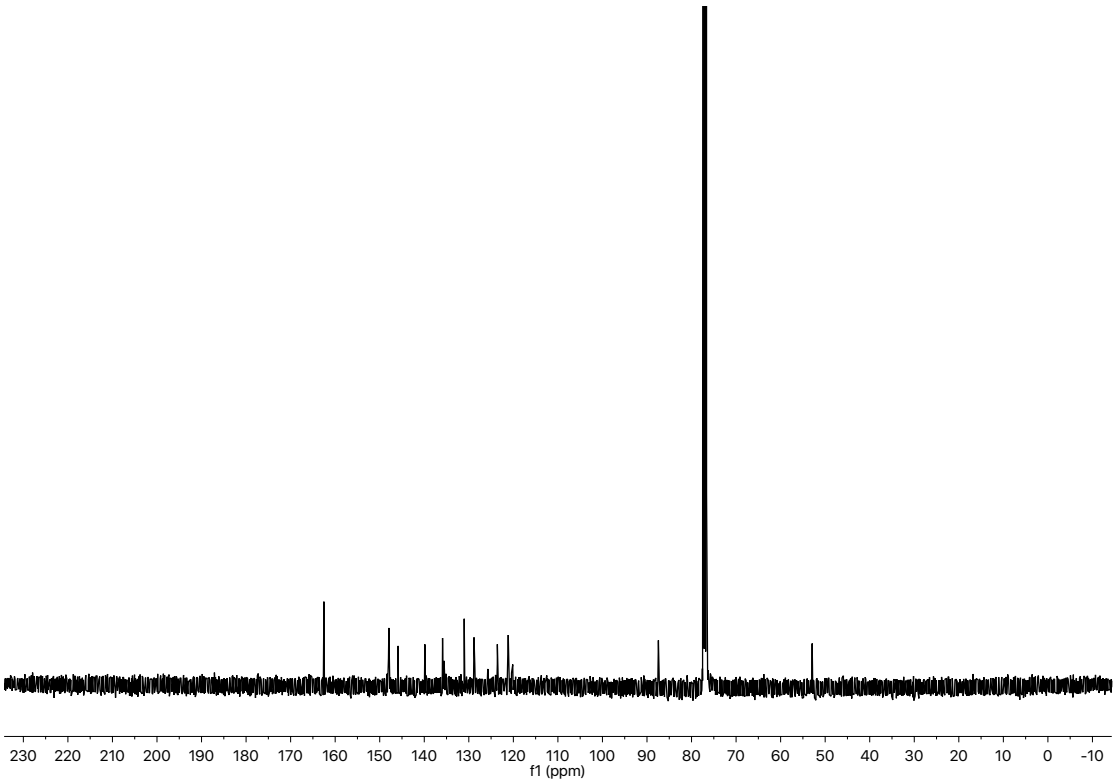

Figure S5. ^{13}C NMR spectrum of ligand **7** at 25 °C in $CDCl_3$.

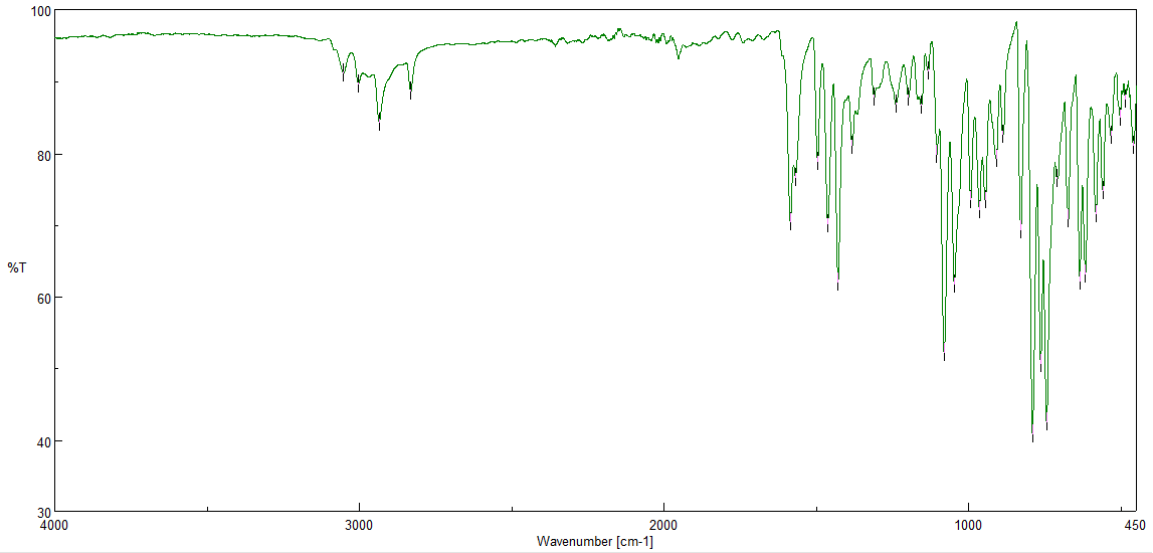

Figure S6. IR spectrum of ligand **7**.

*Complexes **1**, **2**, and related compounds.*

Complex 1.

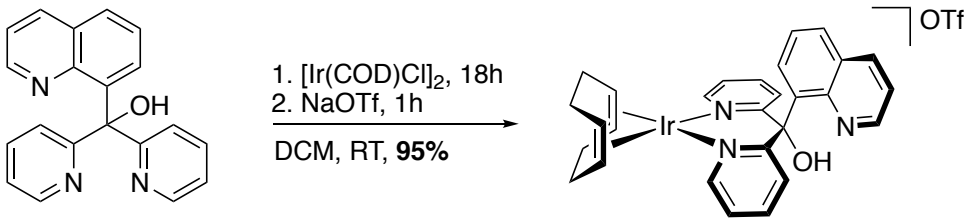

6 **1**

In the glovebox under nitrogen, in a 8 dram vial with magnetic stir bar, chloro(1,5-cyclooctadiene)iridium(I) dimer (50.0 mg, 0.074 mmol, 1 equiv.) and 8-(hydroxydi(pyridin-2-yl)methyl)quinoline **6** (47 mg, 0.148 mmol, 2 equiv.) were dissolved in 3 mL of DCM and left to stirr for 18 hours. After this, sodium trifluoromethanesulfonate (28 mg, 0.163 mmol, 2.2 equiv.) was added to the mixture, which was stirred for 1 hour more. After stirring for 1 hour, the solution was filtered through a Teflon syringe filter to remove insoluble solids. The solvent was evaporated under reduced pressure and yielded a yellow glassy solid. This yellow solid was dissolved in 0.4 mL of dry DCM, then slowly added, to 20 mL of hexanes, leading to precipitation of **1**. A yellow crystalline solid was acquired and dried under vacuum (107 mg, 0.140 mmol, 95%). This sample was later determined to be spectroscopically pure under NMR. Layering of n-heptane over dichloromethane solution of **1** produced crystals suitable for X-ray crystallography.

^{1}H NMR (600 MHz, Dichloromethane-d_2) δ 8.52 (d, J = 5.7 Hz, 2H), 8.40 (dd, J = 4.3, 1.7 Hz, 1H), 8.32 (d, J = 8.1 Hz, 2H), 8.16 (dd, J = 8.2, 1.7 Hz, 1H), 8.09 (td, J = 7.9, 1.4 Hz, 2H), 7.98 (d, J = 8.5 Hz, 1H), 7.49 (dd, J = 8.5, 7.0 Hz, 1H), 7.43 (t, J = 6.7 Hz, 2H), 7.37 (dd, J = 8.2, 4.4 Hz, 1H), 6.89 (d, J = 7.0 Hz, 1H), 5.52 (s, 1H), 3.75 (d, J = 7.4 Hz, 2H), 2.63 – 2.34 (m, 4H), 1.84 (q, J = 8.0 Hz, 2H), 1.63 (s, 2H), 1.47 (d, J = 8.6 Hz, 2H).

^{13}C NMR (101 MHz, Dichloromethane-d_2) δ 149.16, 148.82, 140.14, 136.18, 129.29, 128.93, 128.19, 124.59, 124.18, 123.97, 122.22, 109.76, 31.01 (d, J = 10.7 Hz).

^{19}F NMR (376 MHz, Dichloromethane-d_2) δ -78.94.

FTIR *v* 3359.87, 2912.95, 2884.99, 2840.63, 2357.55, 1604, 1494.08, 1465.15, 1437.67, 1380.78, 1274.72, 1252.06, 1226.02, 1204.33, 1151.78, 1069.82,1027.87, 985.447, 897.219, 828.759, 796.457, 762.709, 696.177, 663.393, 632.537, 571.79, 516.347, 487.902.

MS (MALDI) calculated for $[C_{28}H_{27}IrN_3O]^+$ 614.18, found 613.80.

Anal. Calcd for $C_{29}H_{27}F_3IrN_3O_4S$: C, 45.66; H, 3.57; N, 5.51; S, 4.20 Found: C, 45.51; H, 3.67; N, 5.35; S, 4.22.

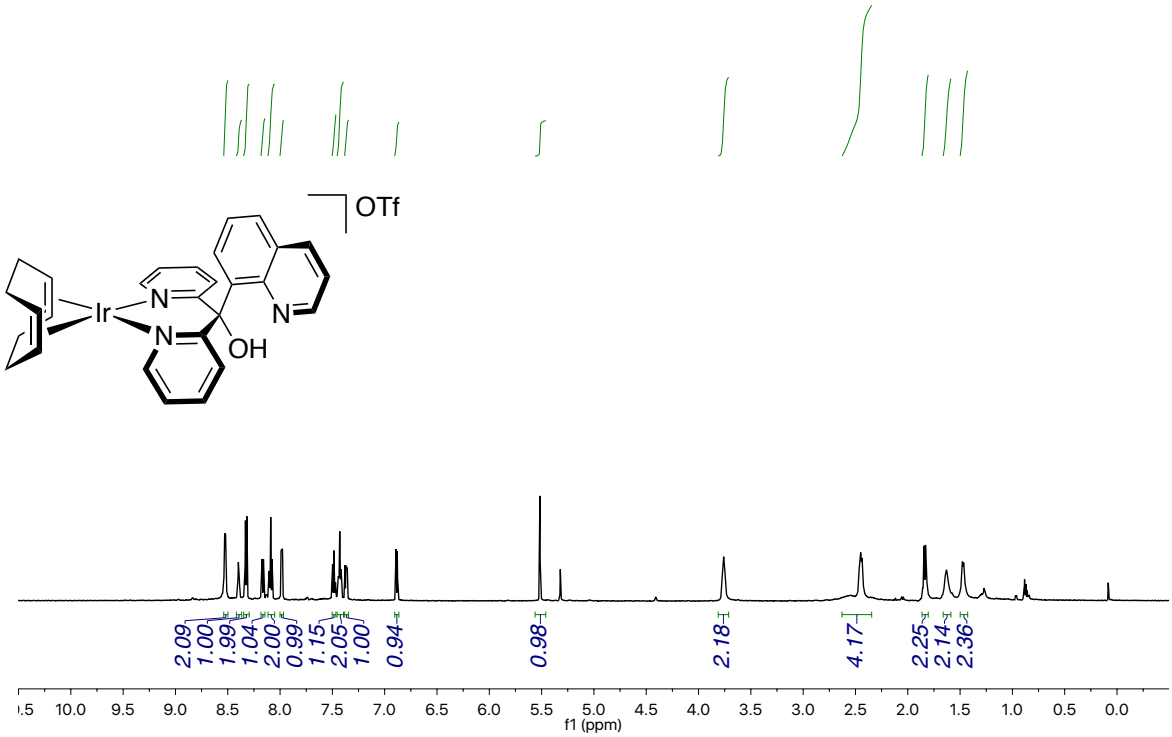

Figure S7. ^{1}H NMR spectrum of Complex **1** at 25 °C in CD_2Cl_2.

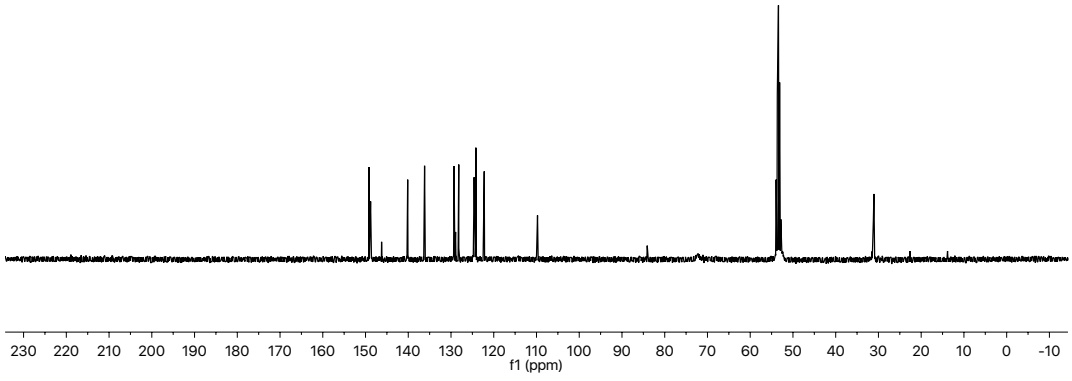

Figure S8. ^{13}C NMR spectrum of Complex **1** at 25 °C in CD_2Cl_2.

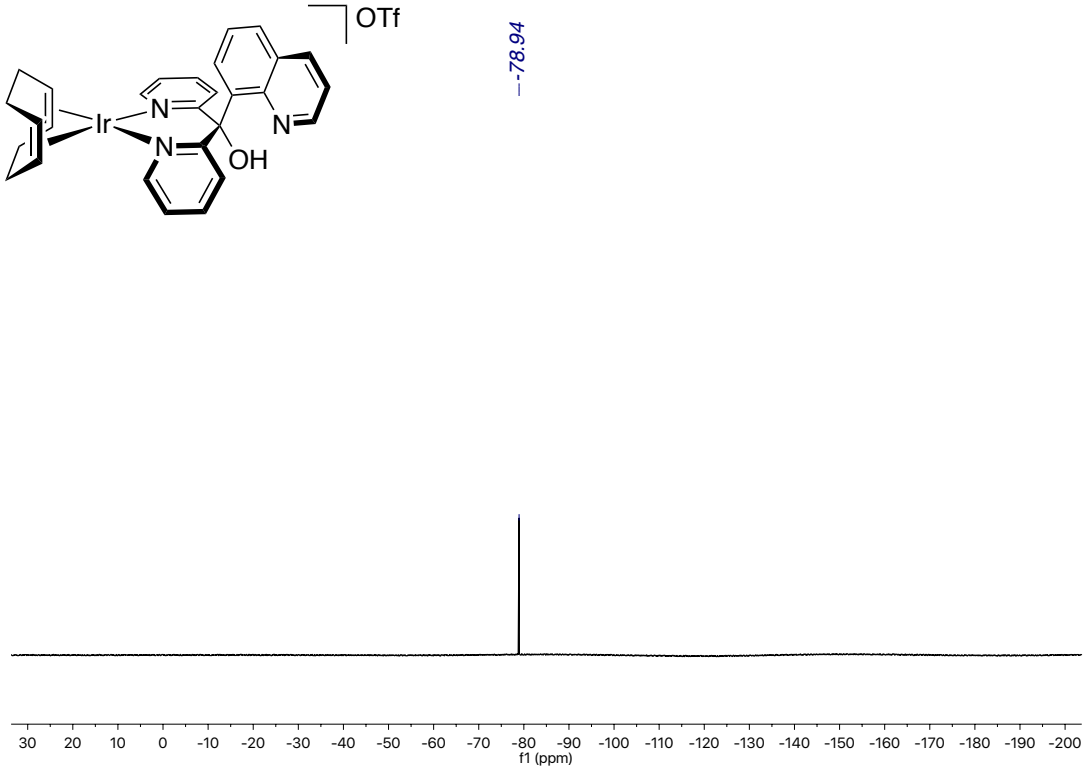

Figure S9. ^{19}F NMR spectrum of Complex **1** at 25 °C in CD_2Cl_2.

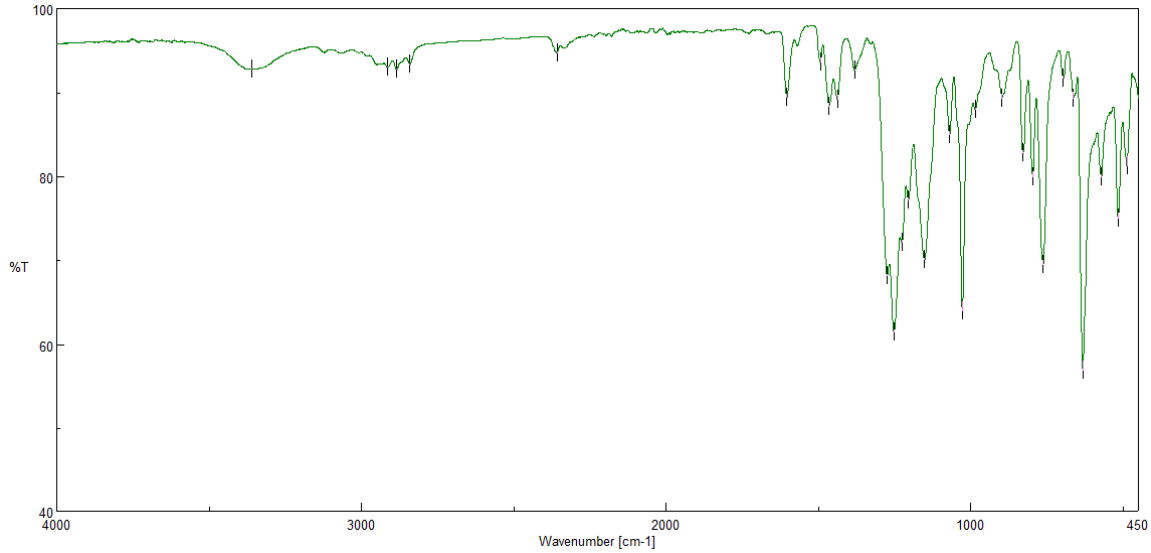

Figure S10. IR spectrum of Complex **1**.

Complex 2.

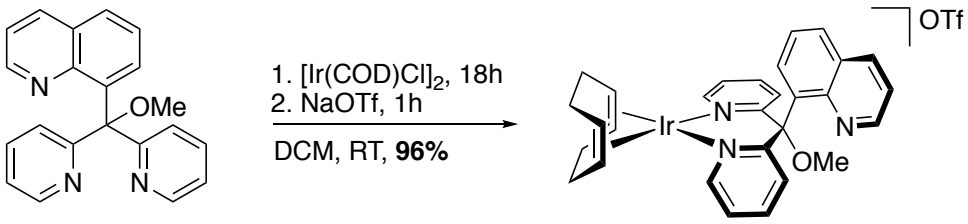

7 **2**

Complex **2** was prepared by following an analogous procedure to that described above for complex **1.** In the glovebox under nitrogen, in a 8 dram vial with magnetic stir bar, chloro(1,5-cyclooctadiene)Iridium(I) dimer (50.0 mg, 0.074 mmol, 1 equiv.) and 8-(methoxydi(pyridin-2-yl)methyl)quinoline **7** (48 mg, 0.148 mmol, 2 equiv.) were dissolved in 3 mL of DCM and left to stirr for 18 hours. Sodium trifluoromethanesulfonate (28 mg, 0.163 mmol, 2.2 equiv.) was then added to the mixture, which was stirred for 1 hour more. After stirring, the solution was filtered through a Teflon syringe filter to remove insoluble. The solvent was evaporated under reduced pressure and yielded in a yellow glassy solid. This yellow solid was dissolved in 0.4 mL of dry DCM, then added slowly, dropwise, to 20 mL of hexanes, leading to precipitation of **2**. A yellow crystalline solid was acquired and dried under vacuum (110 mg, 0.142 mmol, 96%). This sample was later determined to be spectroscopically pure under NMR.

^{1}H NMR (500 MHz, Dichloromethane-d_2) δ 8.74 – 8.70 (m, 1H), 8.40 (d, J = 5.7 Hz, 1H), 8.34 (dt, J = 4.4, 1.5 Hz, 1H), 8.18 – 8.10 (m, 3H), 8.07 – 7.99 (m, 3H), 7.53 (ddt, J = 7.3, 5.8, 1.5 Hz, 1H), 7.49 (ddd, J = 8.2, 6.8, 1.1 Hz, 1H), 7.39 – 7.35 (m, 1H), 7.35 – 7.31 (m, 1H), 6.75 (dt, J = 6.9, 1.2 Hz, 1H), 3.86 (s, 1H), 3.79 (t, J = 7.6 Hz, 1H), 3.52 (s, 1H), 2.94 (d, J = 1.2 Hz, 3H), 2.47 (d, J = 7.3 Hz, 2H), 1.95 (q, J = 8.7, 6.4 Hz, 2H), 1.83 (s, 2H), 1.40 (q, J = 9.6, 7.7 Hz, 1H), 1.28 (d, J = 6.6 Hz, 2H).

^{13}C NMR (101 MHz, Dichloromethane-d2) δ 150.19, 149.00, 148.18, 147.06, 141.10, 139.35, 135.62, 129.74, 128.23, 127.96, 125.28, 124.79, 123.42, 123.01, 122.18, 107.26, 81.05, 77.80, 66.35, 33.65, 32.52, 29.45.

^{19}F NMR (376 MHz, Dichloromethane-d_2) δ -78.94.

FTIR *v* 2948.63, 2837.74, 1603.04, 1462.26, 1445.39, 1387.53, 1260.25, 1221.68, 1148.4, 1087.17, 1028.35, 990.75, 895.773, 832.133, 796.457, 768.012, 677.856, 655.197, 632.537, 570.344, 516.347, 484.045.

MS (MALDI) calculated for $[C_{29}H_{29}IrN_3O]^+$ 628.19, found 627.86.

Anal. Calcd for $C_{29}H_{27}F_3IrN_3O_4S$: C, 46.38; H, 3.76; N, 5.41; S, 4.13 Found: C, 46.45; H, 3.85; N, 5.38; S, 4.11.

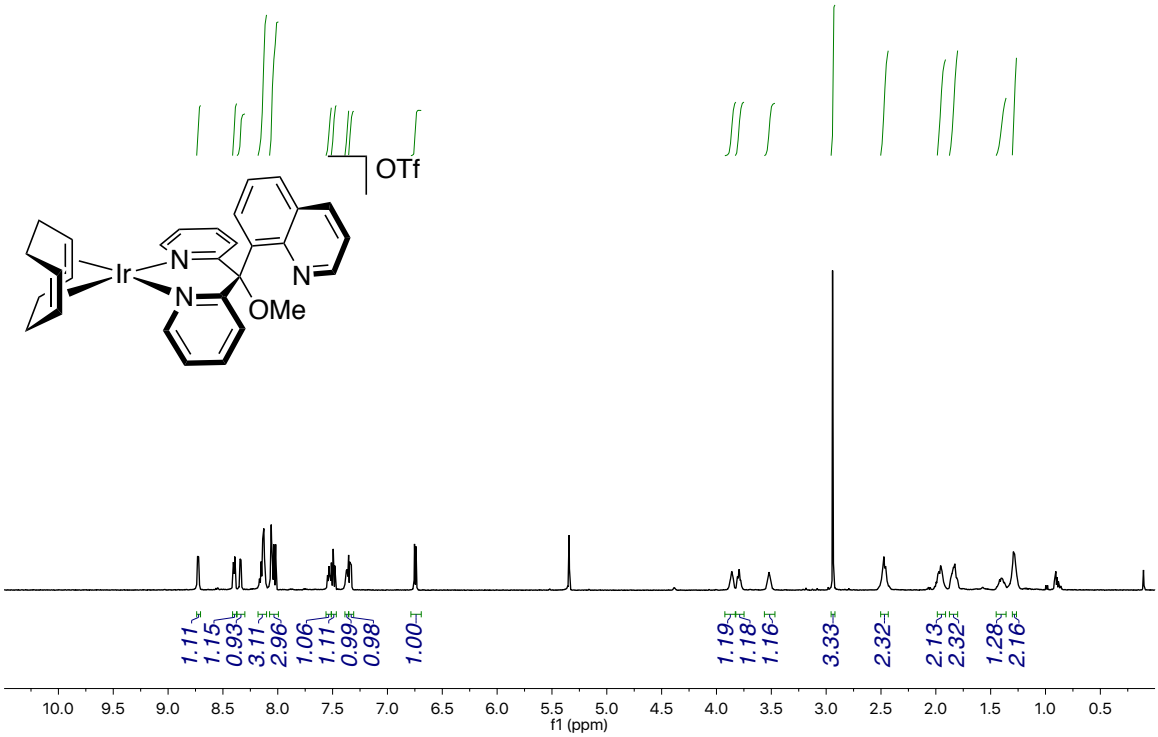

Figure S11. ^{1}H NMR spectrum of Complex **2** at 25 °C in CD_2Cl_2.

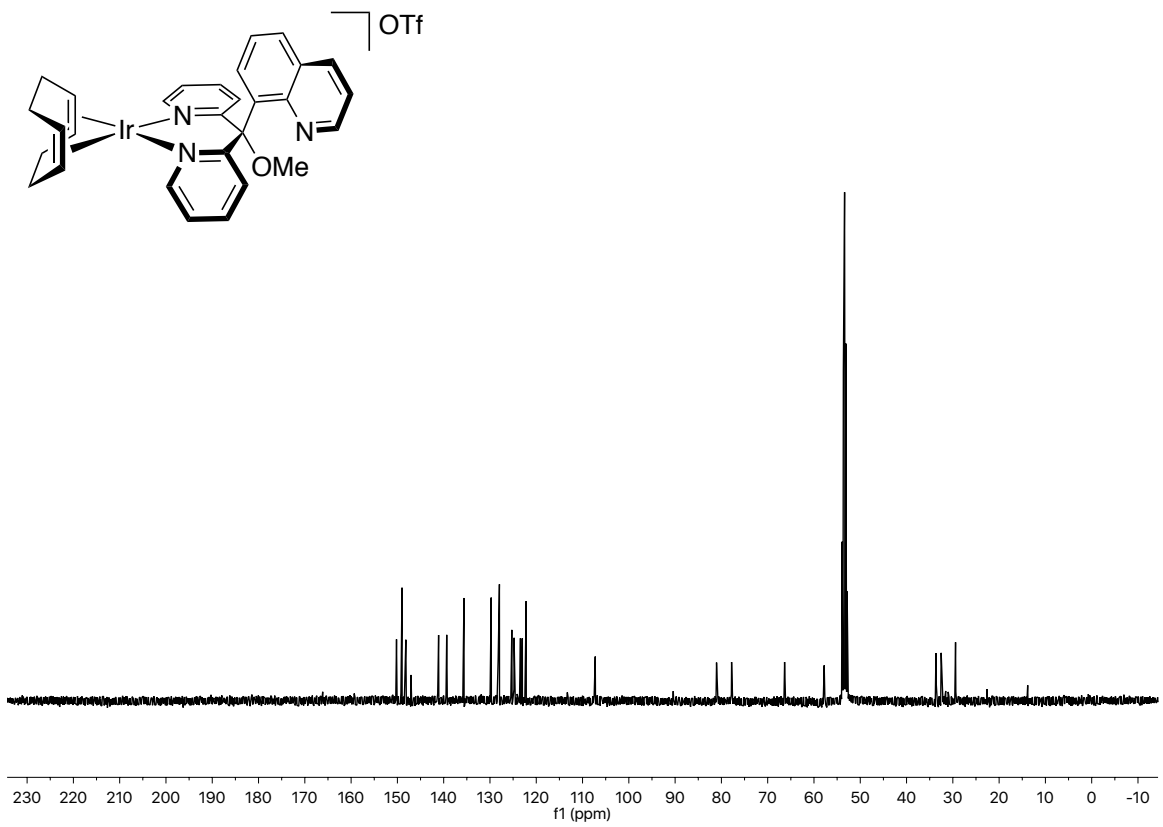

Figure S12. ^{13}C NMR spectrum of Complex **2** at 25 °C in CD_2Cl_2.

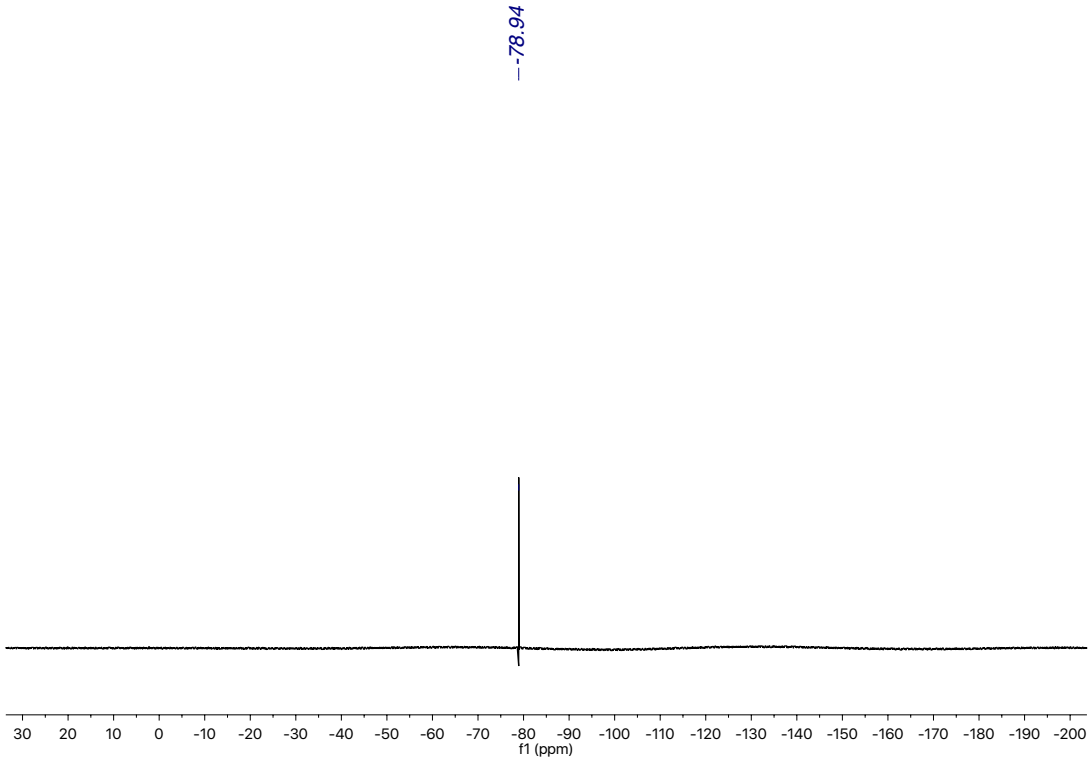

Figure S13. ^{19}F NMR spectrum of Complex **2** at 25 °C in CD_2Cl_2.

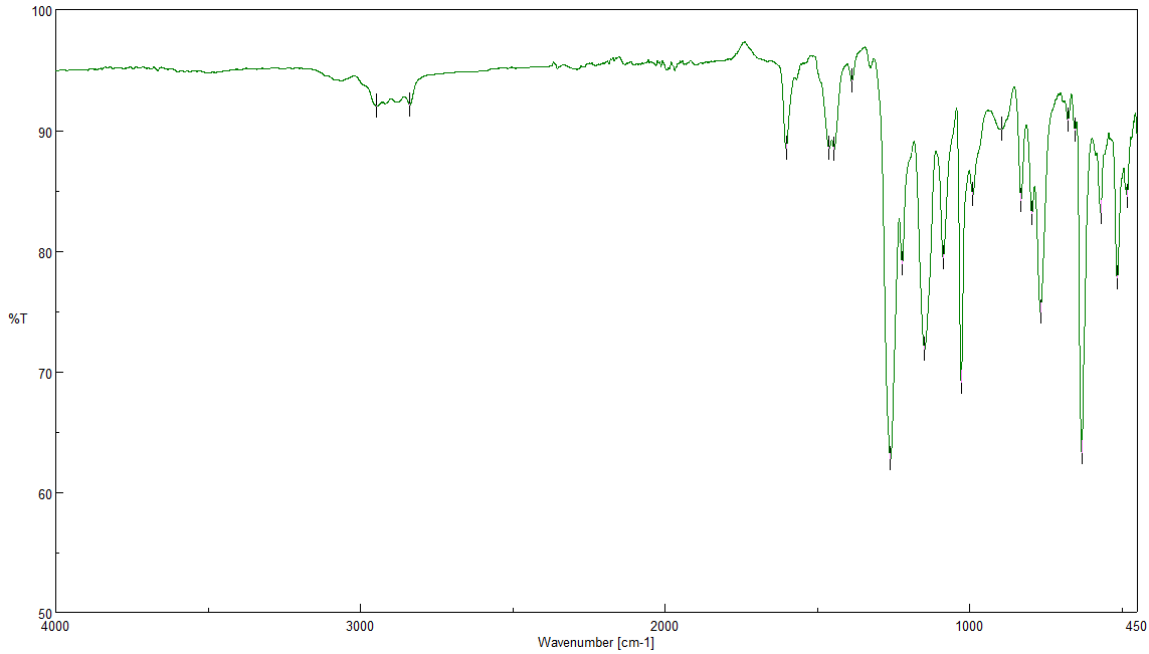

Figure S14. IR spectrum of Complex **2**.

Zn complexes and related compounds.

8-Acetylquinoline (9).

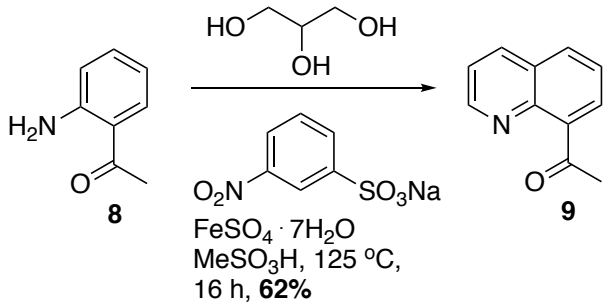

Following a similar procedure to synthesis of 8-bromoquinoline (**4**) described above, 8-acetylquinoline was synthesized by adding 11 mL of methane sulfonic acid to 100 mL 3-neck round bottom flask with magnetic stir bar inside. The flask was heated to 125 °C and 2'-aminoacetophenone (2.70 g, 20.0 mmol, 1 equiv.) was added portionwise over the course of 10 minutes, followed by sodium 3-nitrobenzenesulfonate (2.84 g, 12.6 mmol, 0.63 equiv.) and $FeSO_4 \bullet 7H_2O$ (0.167 g, 0.6 mmol, 0.03 equiv.). Glycerol (3.6 mL, 60.0 mmol, 3 equiv.) was added in two portions (2 × 1.8 mL) using an addition funnel, with 2 hours intervals. After the addition of the second portion of glycerol, the flask was left for 18 hours at 125 °C. The flask was cooled down to room temperature and the brown contents of it were transferred to a 500 mL beaker with the help of 50 mL of water. The content of the beaker was placed in an ice bath and treated with 50% w/v NaOH until pH reached 14. The heterogeneous mixture was extracted three times with diethyl ether (3 × 100 mL). Layer separation appeared to be slow, in some cases over an hour. Combined organic layers where washed with brine, dried with $MgSO_4$, filtered through the Celite pad and evaporated. Obtained brown oil was distilled under vacuum yielding a high viscosity yellow oil (2.12 g, 12.4 mmol, 62%). Obtained product matched reported NMR spectra for 8-acetylquinoline.

^{1}H NMR (400 MHz, Chloroform-*d*) δ 8.98 (ddt, *J* = 3.5, 1.8, 0.9 Hz, 1H), 8.22 – 8.16 (m, 1H), 8.02 – 7.87 (m, 2H), 7.59 (ddt, *J* = 8.2, 7.1, 0.8 Hz, 1H), 7.46 (ddt, *J* = 8.3, 4.2, 0.9 Hz, 1H), 2.95 (d, *J* = 0.7 Hz, 3H).

^{13}C NMR (101 MHz, Chloroform-*d*) δ 150.35, 136.19, 131.25, 129.12, 125.89, 121.34, 32.68.

1-(Pyridin-2-yl)-1-(quinolin-8-yl)ethan-1-ol (10).

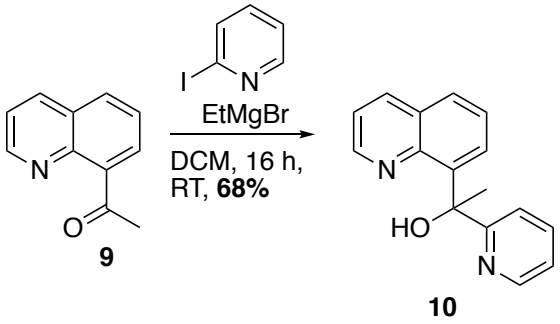

2-Iodopyridine (0.46 mL, 3.56 mmol, 1.5 equiv.) was added to a previously flame dried 250 mL flask with a magnetic stir bar inside of the glove box, followed by the addition of 50 mL of dry DCM. The flask was sealed with the rubber stopper and taken outside of the glove box, later to be connected to the nitrogen line. 3M solution of EtMgBr in diethyl ester (1.2 mL, 3.56 mmol, 1.5 equiv.) in a syringe with a needle was added dropwise to the stirring DCM solution of 2-iodopyridine through the rubber stopper and left for 45 minutes. Solution of 8-acetylquinoline (406 mg, 2.37 mmol, 1 equiv.) in 10 mL of dry DCM was added dropwise in the same way and left for 16 hours. Reaction solution was washed with saturated $NaHCO_3$ solution of 30 mL, which was then extracted twice with DCM (2 × 20 mL). Combined DCM fractions were dried over $MgSO_4$, treated with activated charcoal, filtered through a celite pad and evaporated. The obtained yellow oil underwent recrystallization from boiling diethyl ether resulting in white crystals (403 mg, 1.61 mmol, 68%) that were further analyzed by NMR and proved to be spectroscopically pure.

^{1}H NMR (400 MHz, Chloroform-*d*) δ 8.71 (dt, *J* = 4.4, 1.6 Hz, 2H), 8.41 (dtd, *J* = 4.9, 1.7, 0.9 Hz, 1H), 8.16 (dt, *J* = 8.3, 1.5 Hz, 1H), 7.99 (dq, *J* = 8.0, 1.2 Hz, 1H), 7.86 (dt, *J* = 7.3, 1.3 Hz, 1H), 7.74 (dq, *J* = 8.3, 1.3 Hz, 1H), 7.66 (dddd, *J* = 8.8, 7.9, 2.2, 1.1 Hz, 1H), 7.56 (ddd, *J* = 8.4, 7.3, 1.2 Hz, 1H), 7.36 (ddt, *J* = 8.3, 4.3, 1.2 Hz, 1H), 7.04 (ddt, *J* = 7.5, 4.8, 1.3 Hz, 1H), 2.12 (d, *J* = 1.2 Hz, 3H).

^{13}C NMR (101 MHz, Chloroform-*d*) δ 167.64, 148.08, 147.50 (d, *J* = 6.5 Hz), 146.12, 142.61, 137.36, 136.15, 128.83, 128.14, 127.34, 126.94 – 126.05 (m), 121.12 (d, *J* = 5.7 Hz), 120.52 (d, *J* = 8.7 Hz), 119.91, 79.02, 29.40 (d, *J* = 4.6 Hz).

MS (MALDI) calculated for $C_{16}H_{14}N_2O$ 250.11, found 250.97.

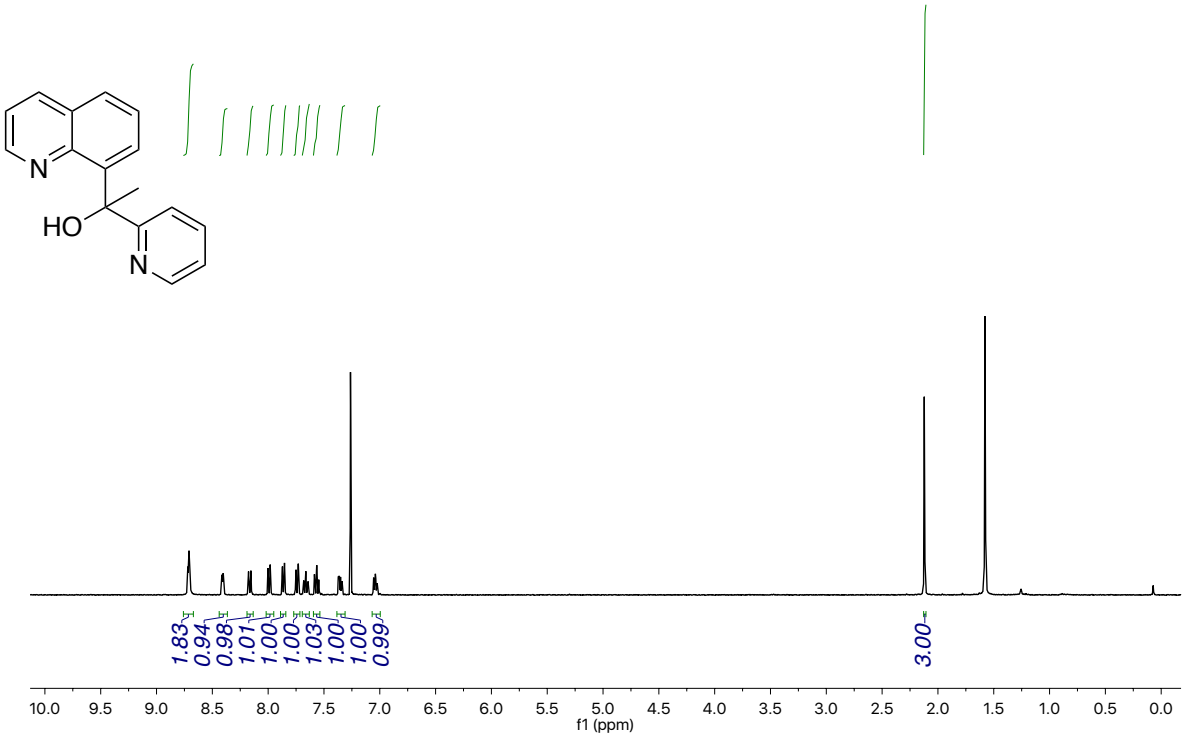

Figure S15. ^{1}H NMR spectrum of **10** at 25 °C in $CDCl_3$.

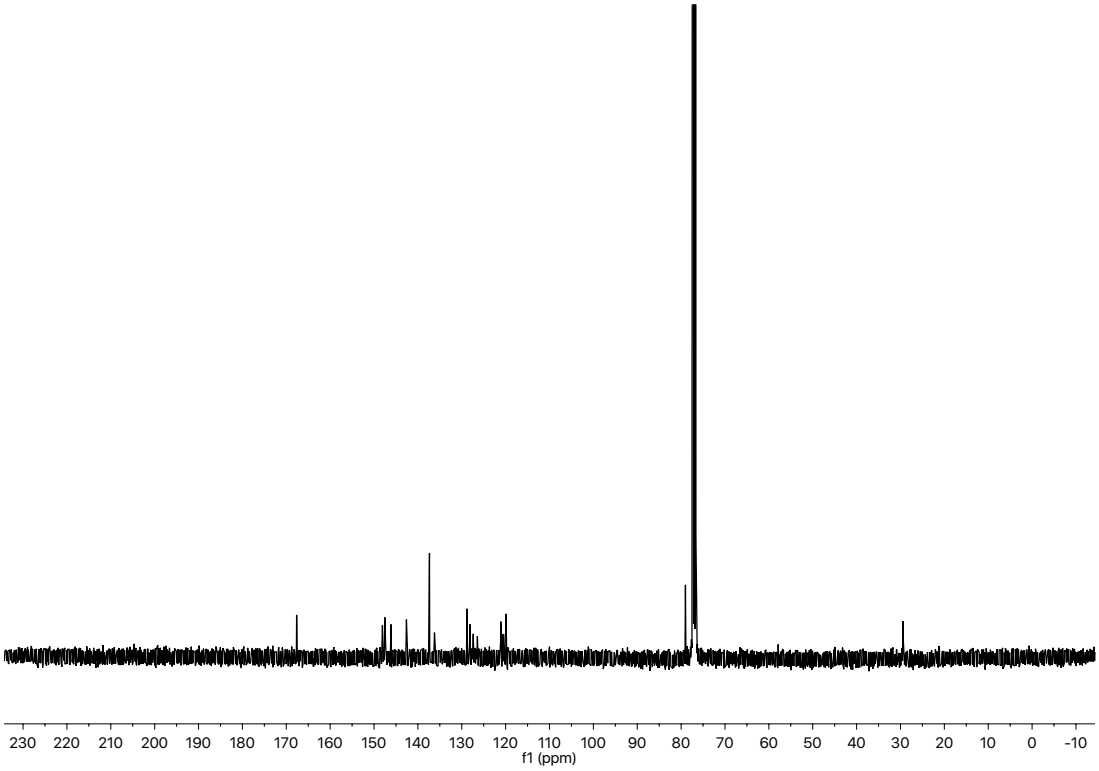

Figure S16. ^{13}C NMR spectrum of **10** at 25 °C in $CDCl_3$.

Zn Complex 11.

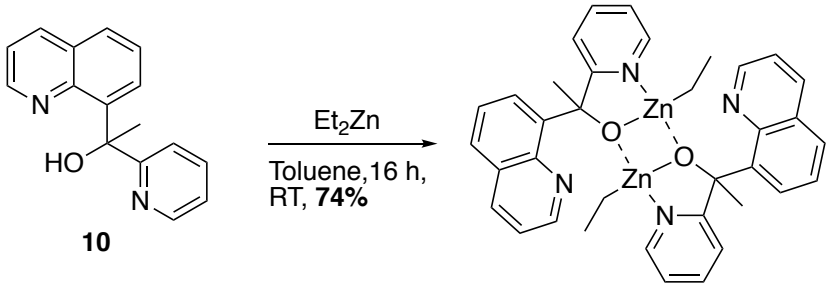

11

In the glovebox under nitrogen, in a 8 dram vial with magnetic stir bar, to solid 1-(pyridin-2-yl)-1-(quinolin-8-yl)ethan-1-ol (**10**) (100 mg, 0.4 mmol, 1 equiv.) was added 0.8 mL toluene solution of diethylzinc (45 μL, 0.4 mmol, 1 equiv.). After this, another 0.4 mL of toluene was added to the mixture and left until white solid precipitated. (Solid precipitation differed from run to run, on average being in between 15-30 minutes.). The obtained solid was washed with toluene on a filter paper and dried under vacuum (203 mg, 0.296 mmol, 74%). The white crystalline solid appeared to be 92% spectroscopically pure under NMR. The remaining impurities may be assigned to the trimeric structure, since both the trimeric and dimeric zinc complexes of similar structure have been previously reported by van Koten et al.,[2] with the dimer being characterized by X-ray crystallography. Layering of n-pentane over benzene solution of **11** produced crystals suitable for X-ray crystallography. These crystals comprised a hydrolysis product, **12**. White crystalline powder of **11** appeared to be relatively air stable over short periods of time, however not tolerant to moisture. If dissolved in organic solvents, **11** appeared to be relatively stable over short periods of time, however unstable if the solution is exposed to air, moisture or light.

^{1}H NMR (400 MHz, Dichloromethane-d_2) δ 8.72 (dd, J = 4.5, 1.9 Hz, 1H), 8.50 (ddd, J = 5.1, 1.7, 1.0 Hz, 1H), 8.24 (ddd, J = 8.3, 1.9, 0.4 Hz, 1H), 8.08 (dd, J = 7.3, 1.5 Hz, 1H), 7.74 (dd, J = 8.2, 1.4 Hz, 1H), 7.67 – 7.55 (m, 2H), 7.46 – 7.38 (m, 2H), 7.18 (ddd, J = 7.4, 5.1, 1.1 Hz, 1H), 2.16 (s, 3H), 1.49 (t, J = 8.1 Hz, 3H), 0.54 (dd, J = 8.0, 3.5 Hz, 2H).

^{13}C NMR (101 MHz, Dichloromethane-d_2) δ 148.52, 145.73, 137.98, 127.72, 126.96 (d, J = 7.7 Hz), 126.76, 121.91, 121.61, 120.58 – 119.63 (m), 31.35, 13.15, -4.60.

FTIR *v* 2977.55, 2925.97, 2885.47, 2849.31, 1597.73, 1566.88, 1494.56, 1463.71, 1430.92, 1358.6, 1294.48, 1233.25, 1166.72, 1130.08, 1098.74, 1082.35, 1054.39, 1017.75, 994.607, 933.378, 916.022, 861.06, 830.205, 788.261, 753.548, 690.391, 638.805, 597.825, 541.417, 507.669, 468.617, 462.832.

MS (MALDI) calculated for $C_{36}H_{36}N_4O_2Zn_2$ 684.14, found 685.35.

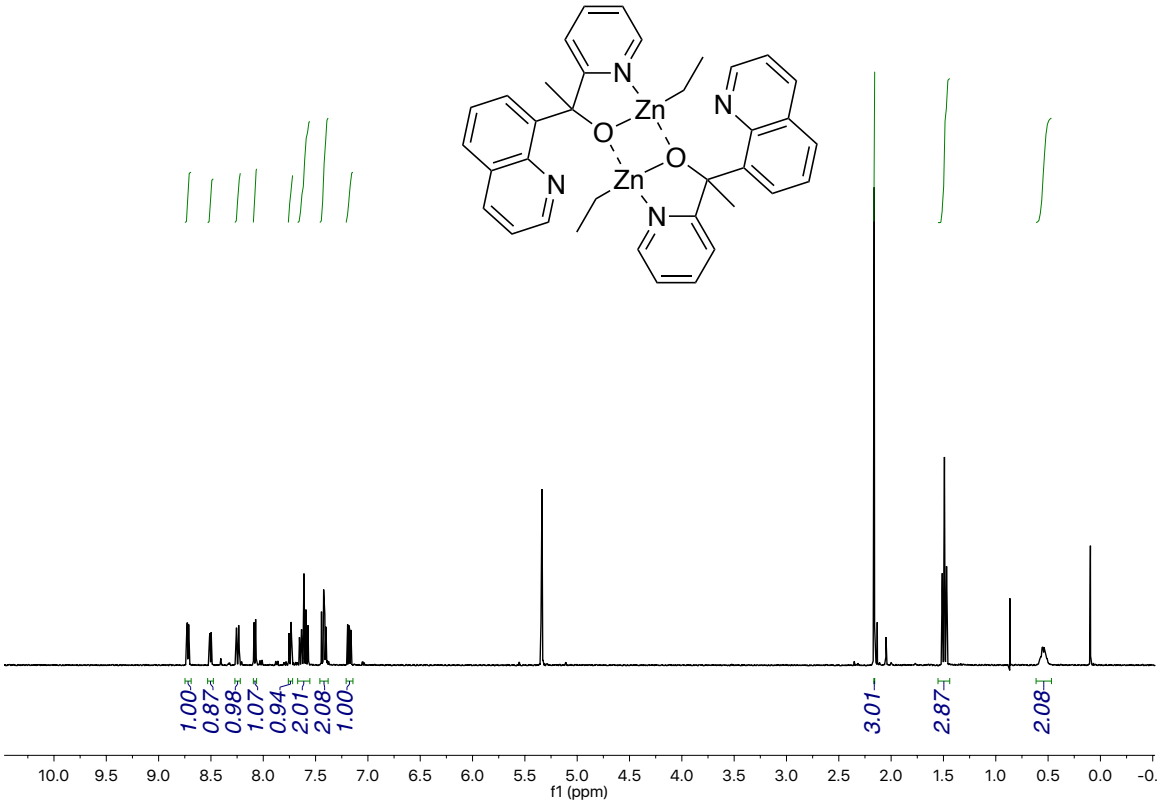

Figure S17. ^{1}H NMR spectrum of **11** at 25 °C in CD_2Cl_2.

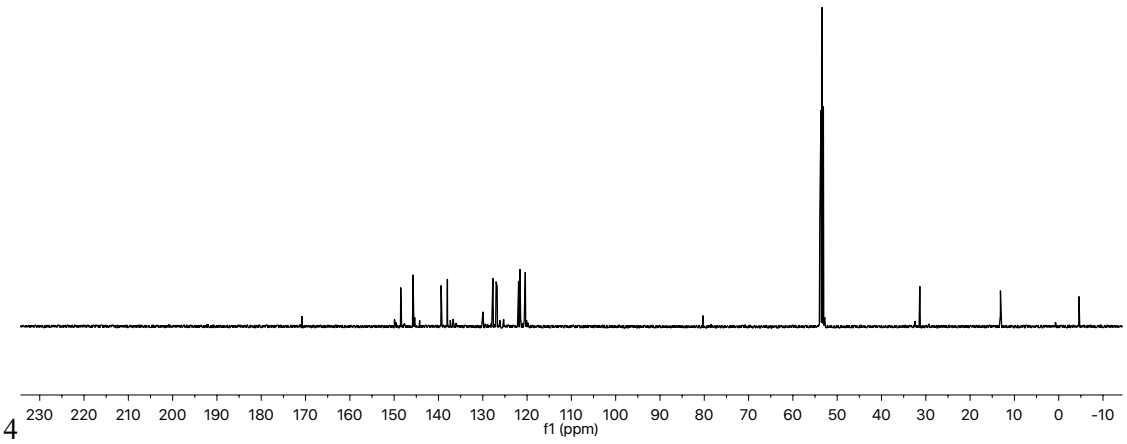

4

Figure S18. ^{13}C NMR spectrum of **11** at 25 °C in CD_2Cl_2.

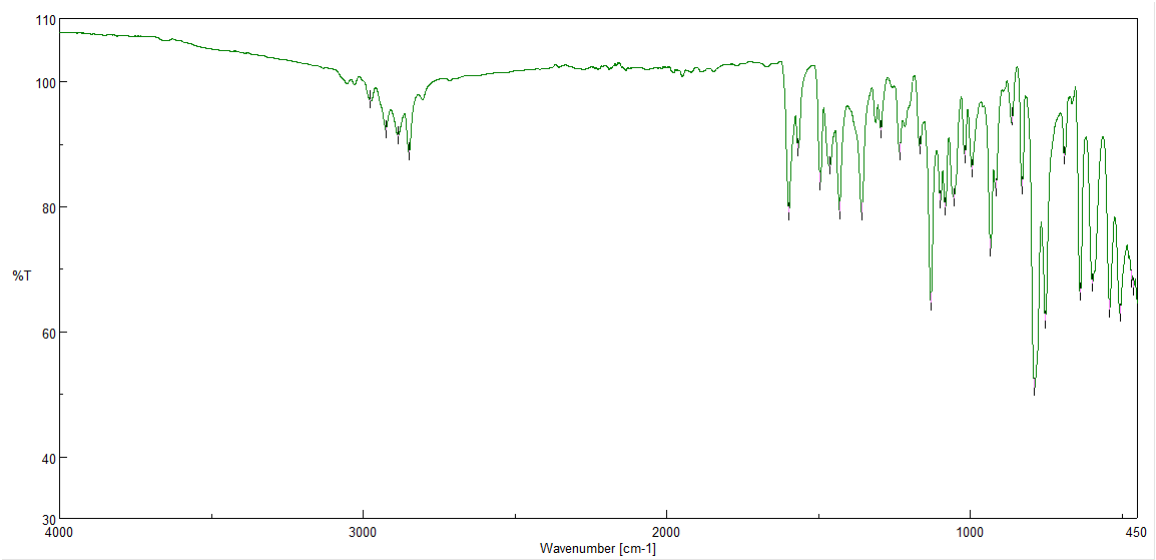

Figure S19. IR spectrum of Complex **11**.

Zn Complex 12.

Crystallization of complex **11** in air results in hydrolysis of **11**'s (ethyl)zinc fragments, ultimately to give complex **12**, which was characterized by single-crystal X-ray diffraction (vide infra).

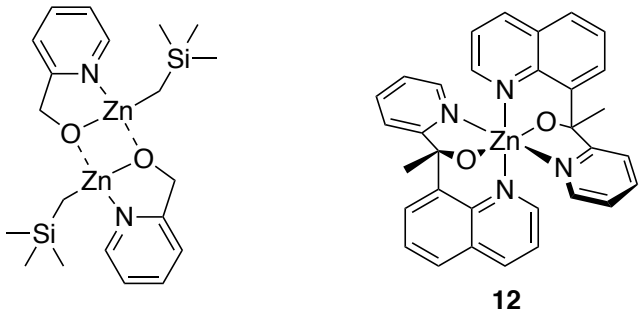

Figure S20. Left: Dimeric zinc complex characterized by van Koten et al.[2] Right: Structure of decomposition product **12**.

S3. Optical Spectral Data

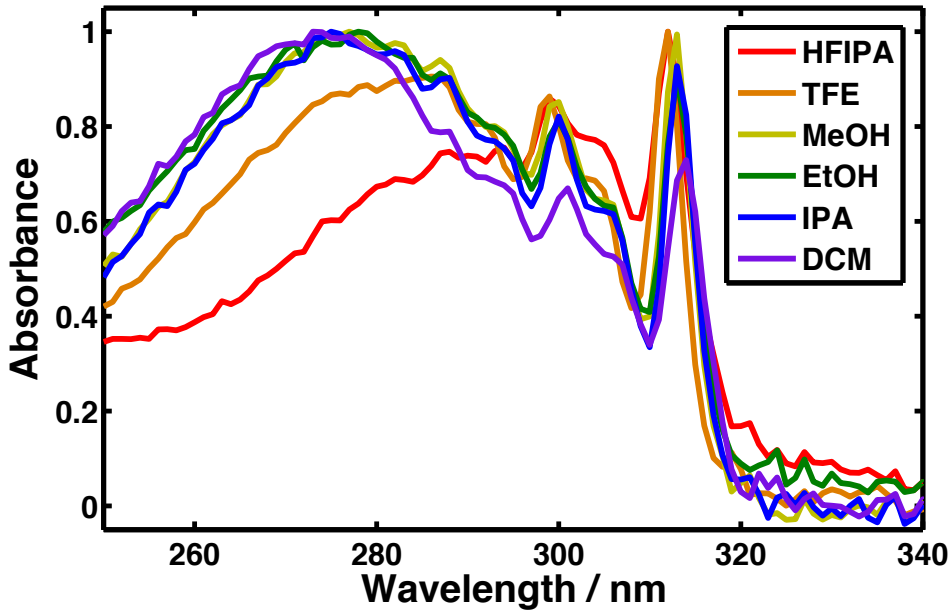

Figure S21. Absorption spectra of quinoline in different solvents.

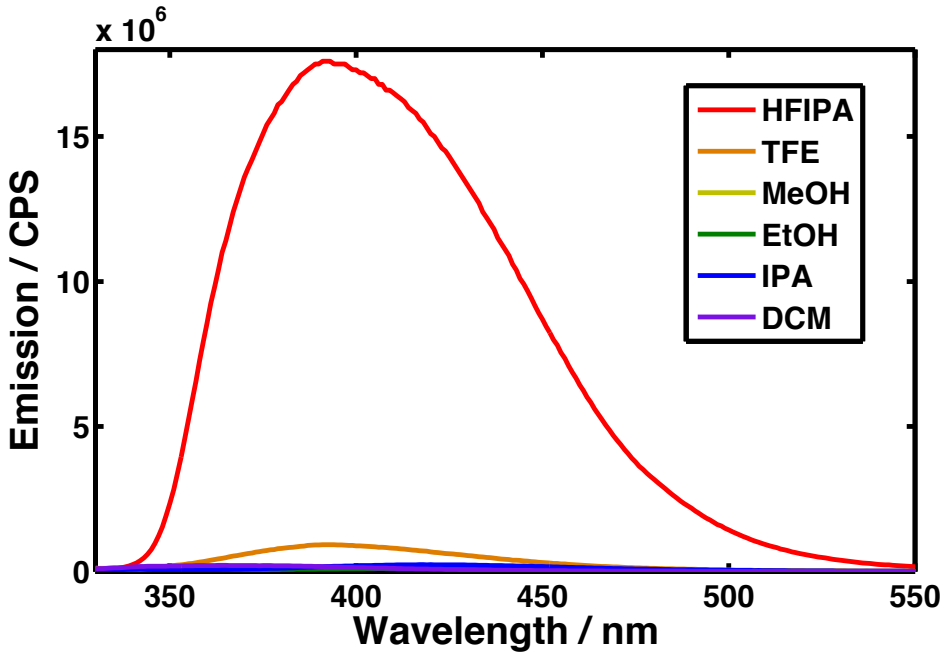

Figure S22. Emission spectra of quinoline in different solvents (310 nm excitation wavelength).

Discussion of Fluorescence and Inter-System Crossing in Quinoline

In general, quinoline displays rapid (< 1 ps) intersystem crossing in the free base form in solution, so it has negligible fluorescence. The protonated form does not undergo intersystem crossing under the same conditions and therefore emits much more strongly. Any quinoline molecule that captures a proton before intersystem crossing occurs will emit from the protonated state. If quinoline is not protonated in the ground state, emission from the protonated form is indicative of excited state proton capture (photobasicity). According to the figures above, quinoline appears to deprotonate both HFIPA and TFE in the excited state. However, emission intensity in HFIPA is significantly stronger than it is in TFE.

Free energy relationships (correlations between the thermodynamics of a reaction and the kinetics of the reaction) have been described throughout the excited state proton transfer community. Generally, proton transfer reactions with greater thermodynamic drive tend to happen more quickly than proton transfer reactions with lower thermodynamic drives. This trend has been well-described in the literature using Marcus free energy relations for proton transfer.[3,4] According to this logic, proton transfer in TFE (pKa = 12.4) should be slower than in HFIPA (pKa = 9.3) when the same excited state proton acceptor is utilized because of the smaller thermodynamic drive for protonation in TFE.

We find that quinoline undergoes rapid ISC that prevents emission, and the only emission we observe comes from quinoline molecules that are protonated before ISC occurs. Therefore, if the excited state proton transfer occurs more quickly, more quinoline get protonated before ISC occurs and there is more emission. Therefore, the greater emission intensity in HFIPA than in TFE is completely consistent with their relative pKa values and the Marcus free energy relations for proton transfer used in the proton transfer literature.

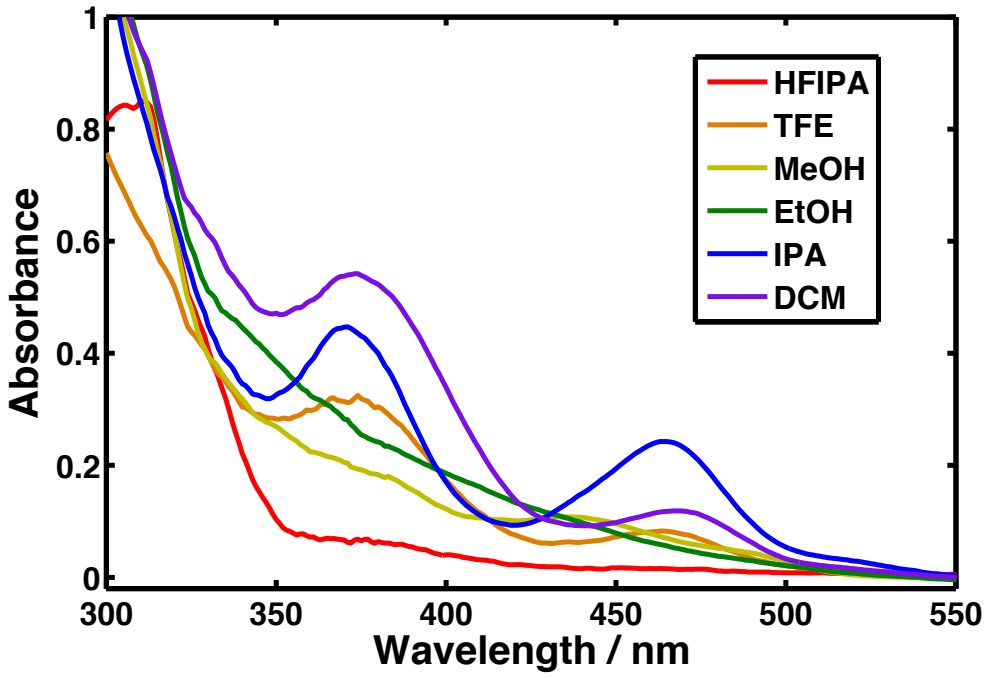

Figure S23. Absorption spectra of complex **1** in different solvents.

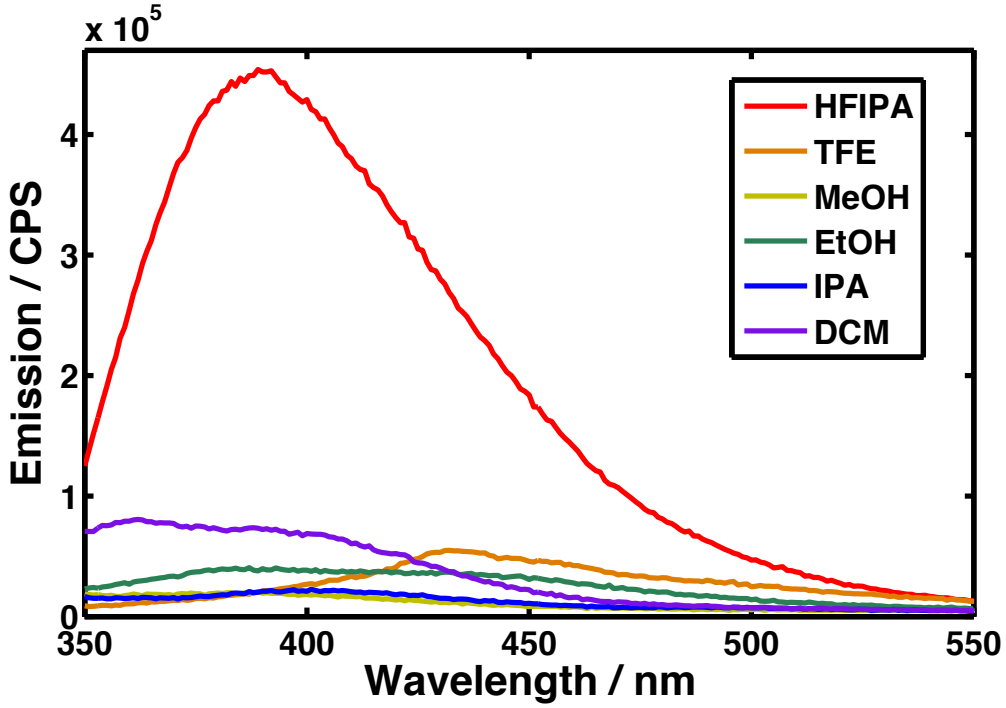

Figure S24. Emission spectra of complex **1** in different solvents (310 nm excitation wavelength).

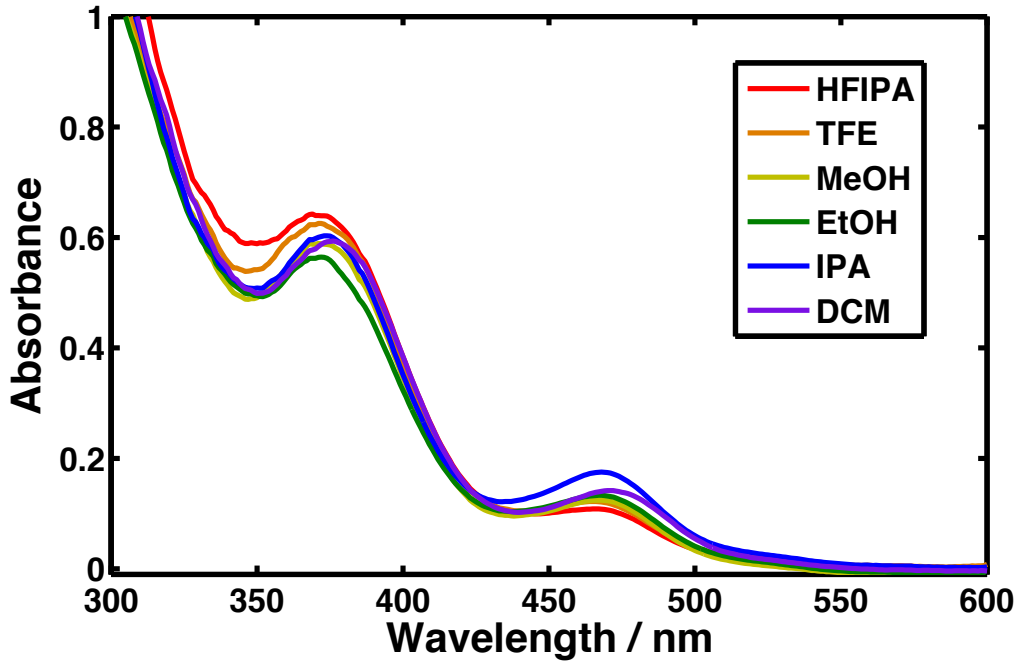

Figure S25. Absorption spectra of complex **2** in different solvents.

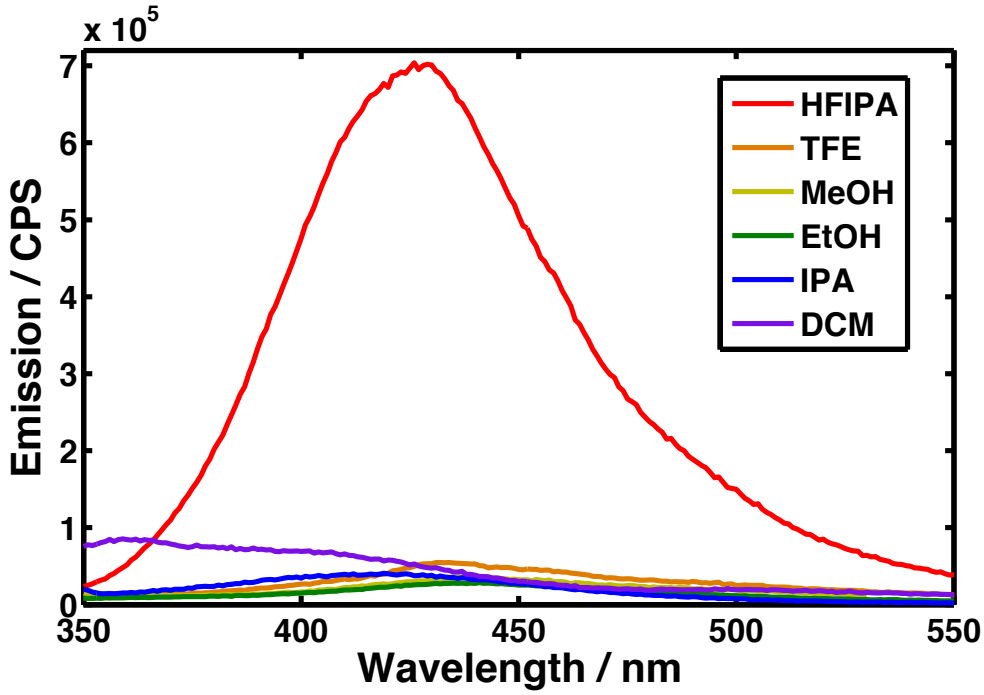

Figure S26. Emission spectra of complex **2** in different solvents (310 nm excitation wavelength).

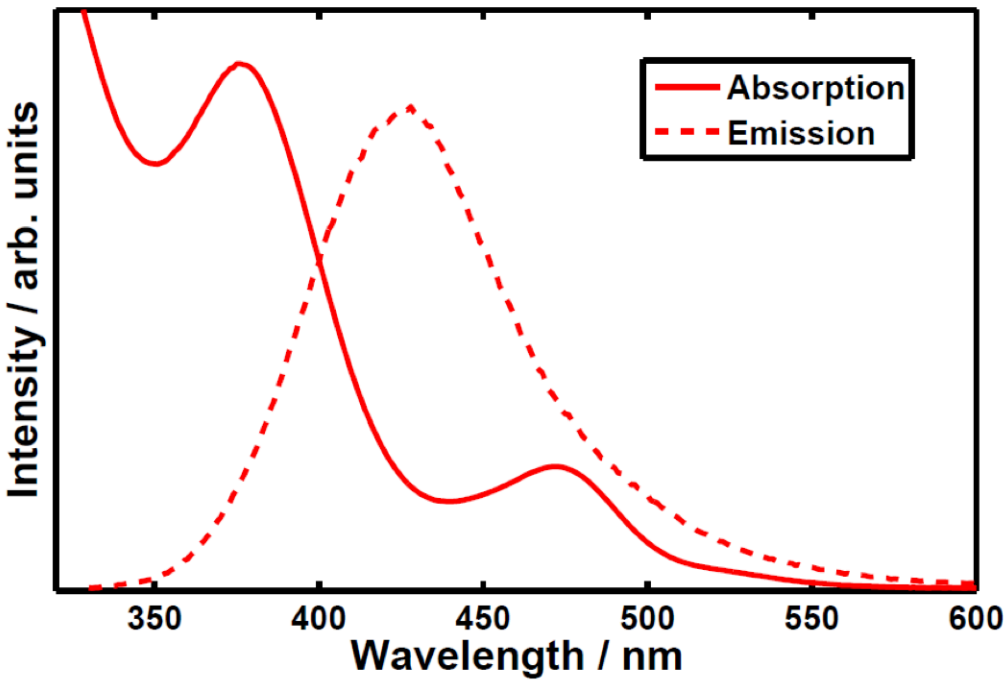

Figure S27. Emission and absorption spectra of complex **2** in HFIPA.

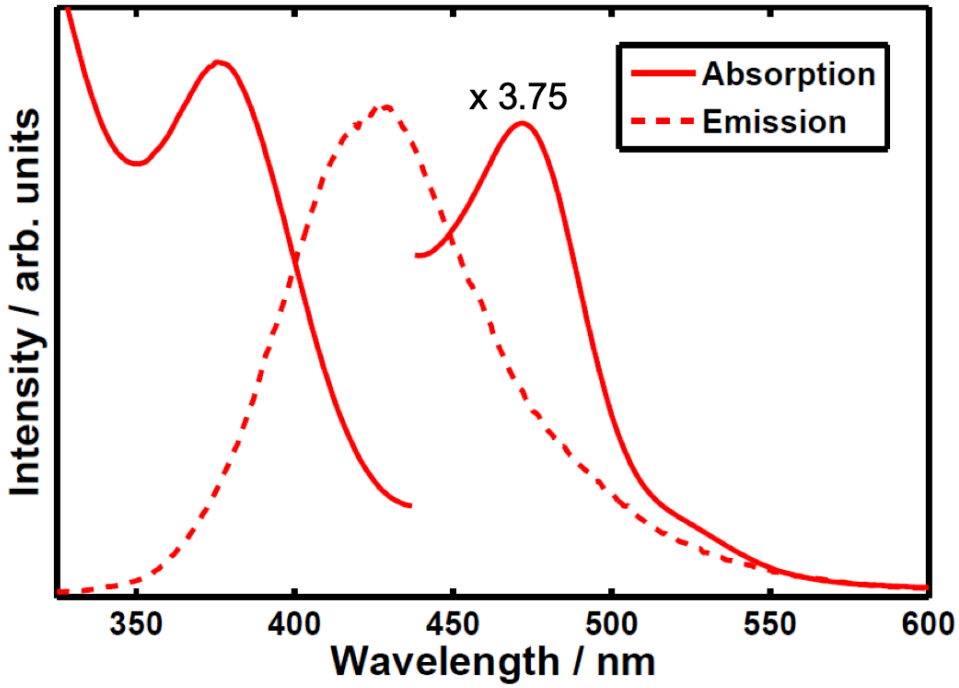

Figure S28. Emission and absorption spectra of complex **2** in HFIPA (absorption region zoomed).

Discussion of UV-visible spectrum of the methyl homolog (complex 13) of complex 2.

We attempted to synthesize the methyl homolog of complex **2** by following an analogous synthetic route, however were not able to isolate clean complex **13**. We suspect that this complex is dynamic in solution. The reaction is frustrated by a ca. 10 mol% impurity (Figure S30). Even though we were not able to separate **13** from its impurity, its UV-visible spectrum showed us that the absorption of complex **2** red-shifts relative to **13** in the presence of quinoline, however, emission spectra of **2** nearly match that of molecular quinoline and show a trend based on solvent pKa values. Therefore, while quinoline may have a polarizing influence on the MLCT and d-d transitions resulting in their red shift, the deprotonation effect seems to be localized on the quinoline moiety.

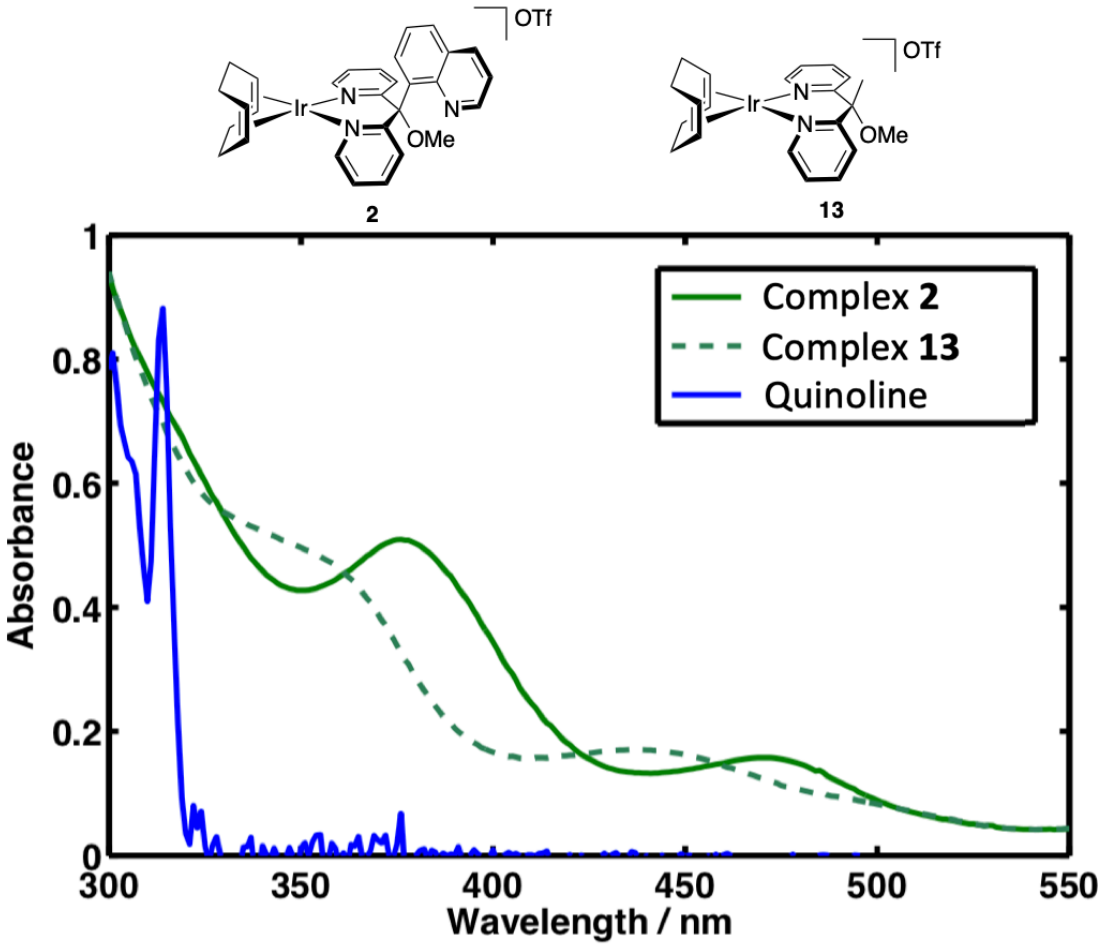

Figure S29. Absorption spectra of complex **2**, complex **13**, and quinoline in DCM.

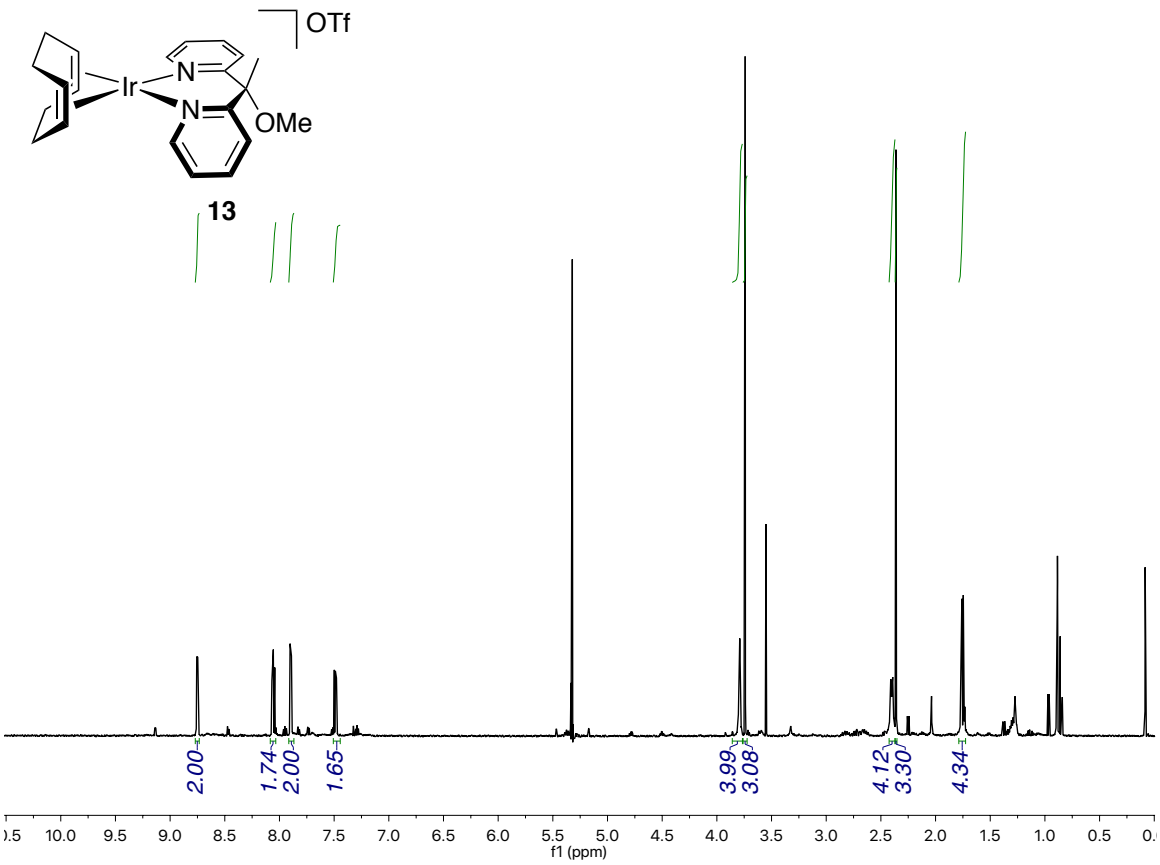

Figure S30. ^{1}H NMR spectrum of Complex **13** at 25 °C in CD_2Cl_2.

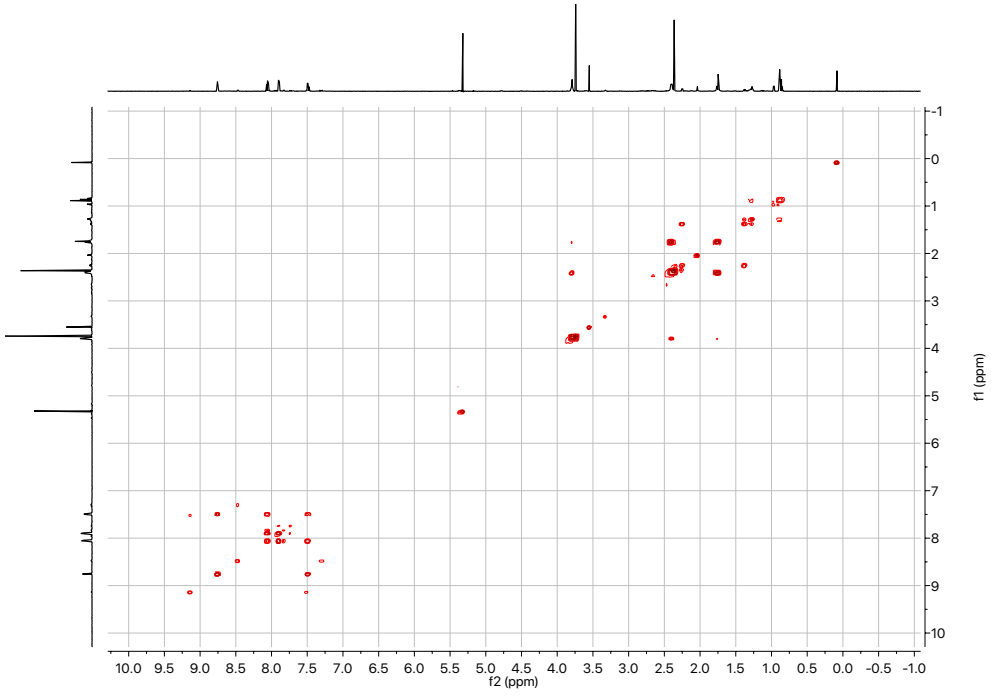

Figure S31. COSY spectrum of Complex **13** at 25 °C in CD_2Cl_2.

S4. Quantum Yield Data.

Table S1. Quantum yield data.

Solvent	Fluorescence Quantum Yield of Quinoline Moiety of Complex **2**
HFIPA	2.8×10^{-3}
TFE	3.2×10^{-4}
MeOH	2.0×10^{-4}
EtOH	1.8×10^{-4}
IPA	2.3×10^{-4}
DCM	6.2×10^{-4}

Fluorescence quantum yields were determined for the quinoline moiety of complex **2** (1.4×10^{-4} M) in various solvents with respect to anthracene (5×10^{-5} M) in ethanol using the equation

$$\Phi = \Phi_R * \frac{Int}{Int_R} * \frac{(1 - 10^{-A_R})}{(1 - 10^{-A})} * \frac{n^2}{{n_R}^2}$$

where Φ is the fluorescence quantum yield, *Int* is the integrated emission intensity, *A* is the absorbance at the excitation wavelength (310 nm in all cases), and *n* is the refractive index of the solvent. The subscript "R" indicates that the values are for the reference chromophore (in this case $\Phi_R = 0.270$[5] and $n_R = 1.361$ for anthracene in ethanol).

Emission spectra were integrated numerically using Simpson's rule.

The absorbance values used for estimation of quantum yield are the absorbance values of complex **2** at 310 nm. Because we know that the absorption at 310 nm may not be entirely due to absorption of the quinoline moiety, the fluorescence quantum yields listed above should be considered as lower bounds for the true quantum yields of the quinoline moiety of complex **2** in the given solvent.

Additionally, due to the overlap of quinoline moiety emission and absorption from LMCT, there is likely to be some re-absorption of emitted photons. Re-absorption of emitted photons would similarly result in an underestimated fluorescence quantum yield.

S5. Complex 1 Decomposition Studies.

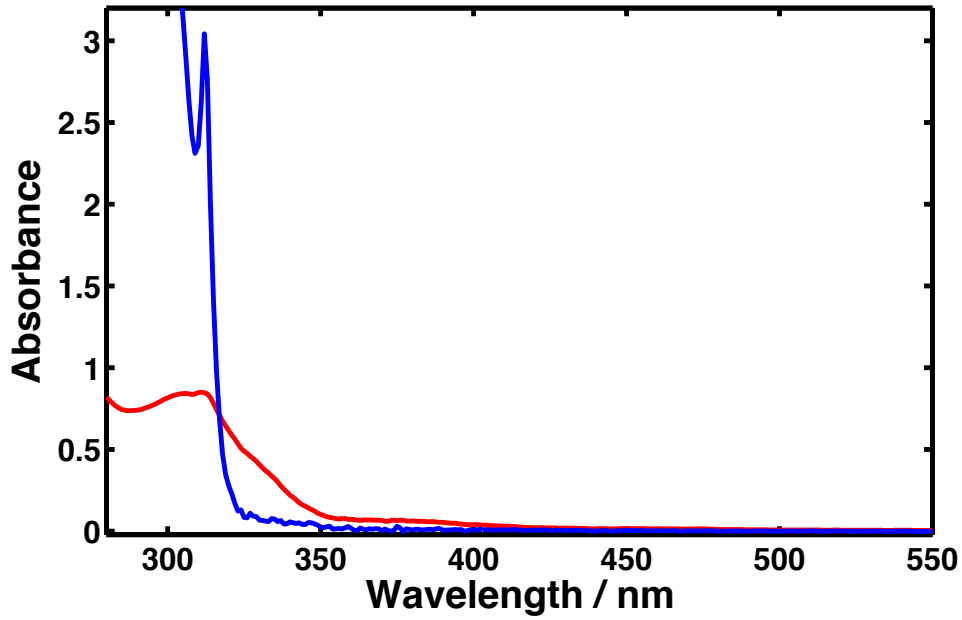

Figure S32. Absorption spectra of complex **1** (red) and ligand **6** (blue) in HFIPA.

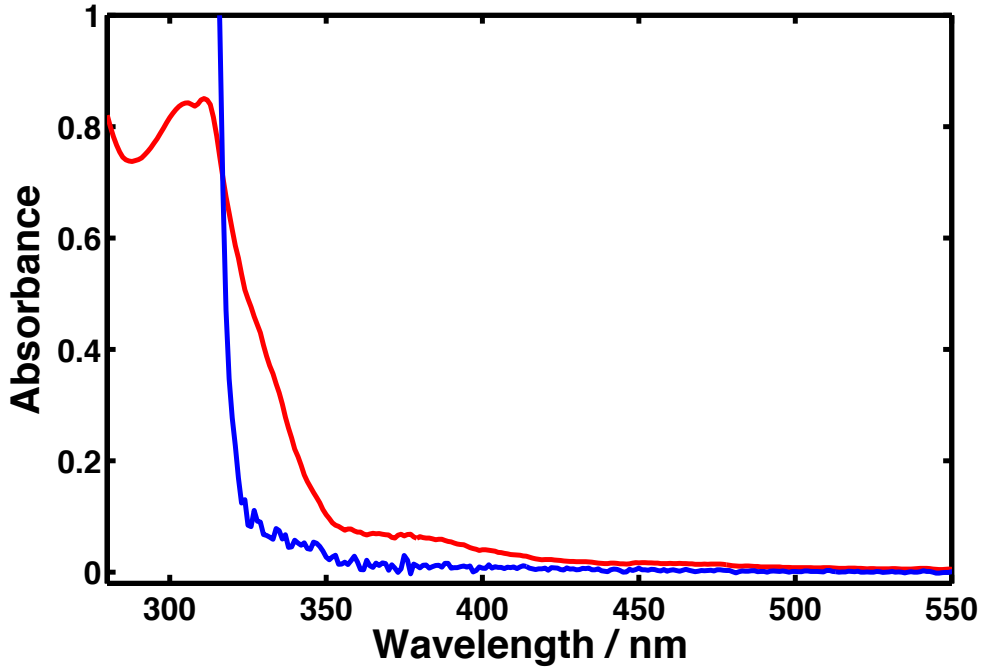

Figure S33. Zoomed absorption spectra of complex **1** (red) and ligand **6** (blue) in HFIPA.

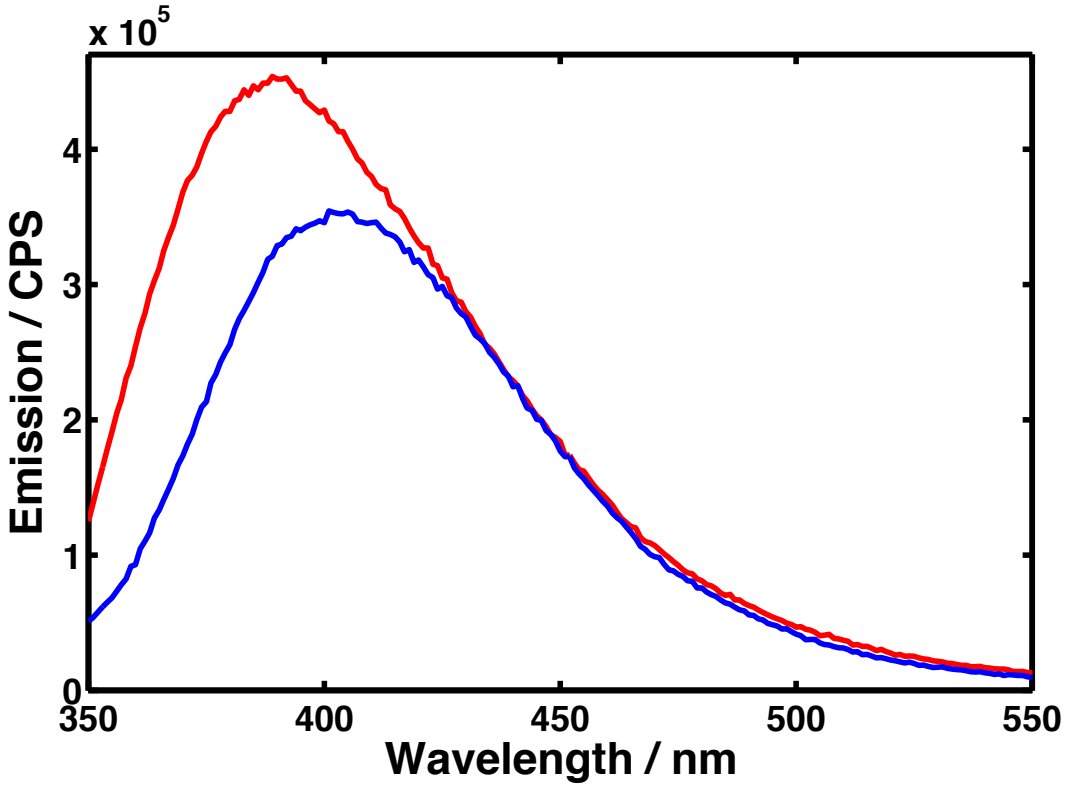

Figure S34. Emission spectra of complex **1** (red) and ligand **6** (blue) in HFIPA (310nm excitation wavelength).

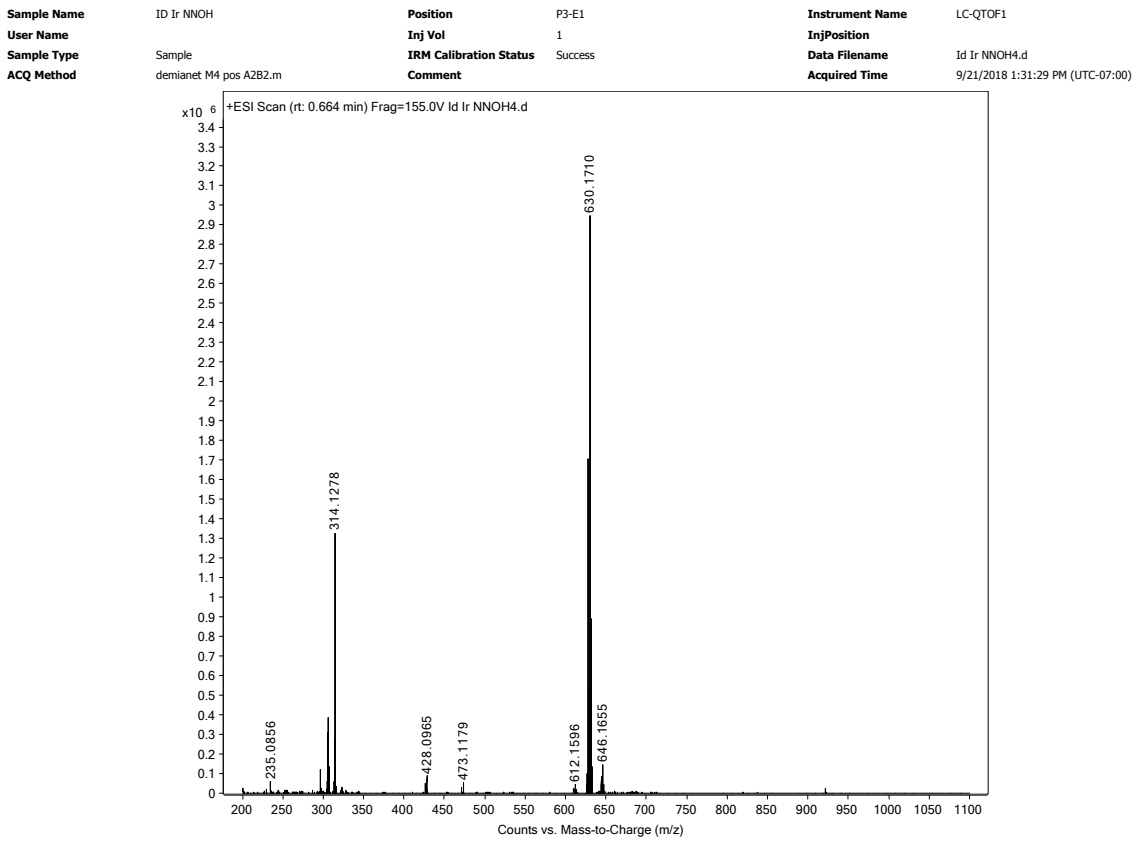

Figure S35. Q-Tof spectra of complex **1** in HFIPA.

S6. Crystal Structure Data

*Crystal Structure Report for Complex **1**.*

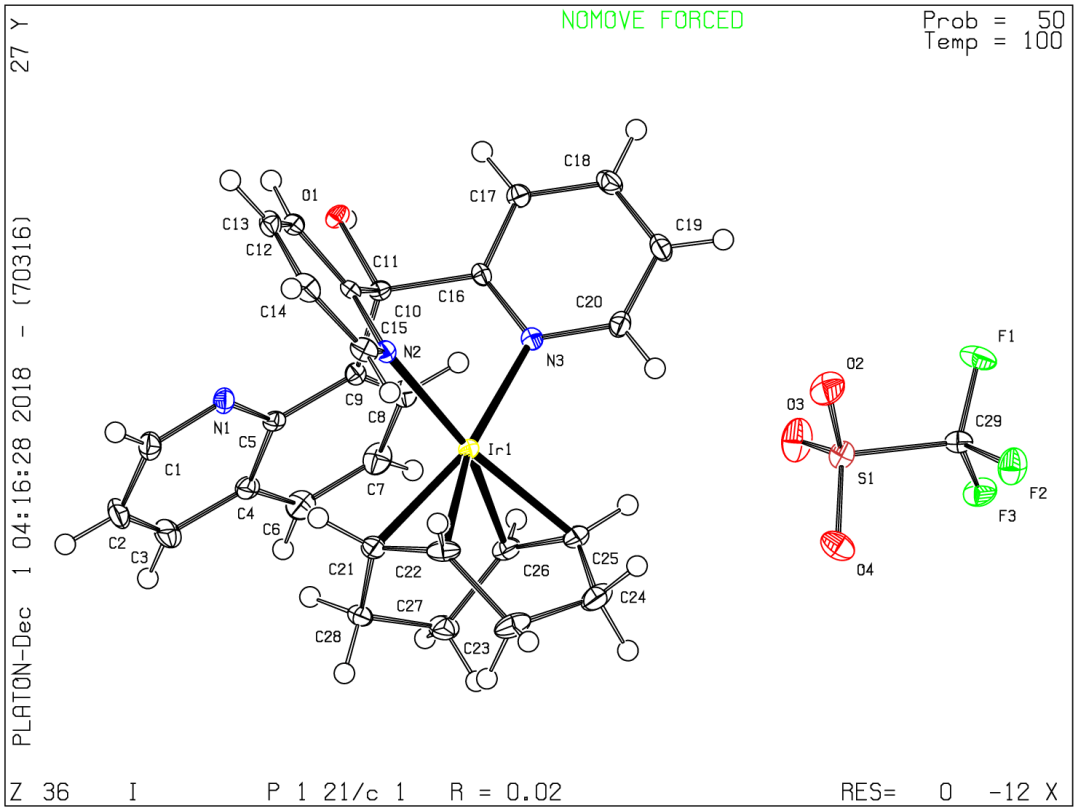

Figure S36. ORTEP diagram of **1**.

Description of Crystallography

A clear red block-like specimen of $C_{29}H_{27}F_3IrN_3O_4S$, approximate dimensions 0.142 mm x 0.203 mm x 0.302 mm, was used for the X-ray crystallographic analysis. The X-ray intensity data were measured on a Bruker APEX DUO system equipped with a TRIUMPH curved-crystal monochromator and a MoKα fine-focus tube (λ = 0.71073 Å).

A total of 2520 frames were collected. The total exposure time was 0.70 hours. The frames were integrated with the Bruker SAINT software package using a SAINT V8.34A (Bruker AXS, 2013) algorithm. The integration of the data using a monoclinic unit cell yielded a total of 65072 reflections to a maximum θ angle of 30.46° (0.70 Å resolution), of which 8003 were independent (average redundancy 8.131, completeness = 99.6%, R_{int} = 7.23%, R_{sig} = 4.07%) and 6740 (84.22%) were greater than $2\sigma(F^2)$. The final cell constants of a = 9.7042(13) Å, b = 14.975(2) Å, c = 18.313(2) Å, β = 96.560(2)°, volume = 2643.8(6) $Å^3$, are based upon the refinement of the XYZ-centroids of 9464 reflections above 20 σ(I) with 4.477°

< 2θ < 60.78°. Data were corrected for absorption effects using the multi-scan method (SADABS). The ratio of minimum to maximum apparent transmission was 0.784. The calculated minimum and maximum transmission coefficients (based on crystal size) are 0.3030 and 0.5260.

The structure was solved and refined using the Bruker SHELXTL Software Package, using the space group P 1 21/c 1, with Z = 4 for the formula unit, $C_{29}H_{27}F_3IrN_3O_4S$. The final anisotropic full-matrix least-squares refinement on F^2 with 385 variables converged at R1 = 2.39%, for the observed data and wR2 = 5.07% for all data. The goodness-of-fit was 1.038. The largest peak in the final difference electron density synthesis was 0.729 $e^-/Å^3$ and the largest hole was -0.635 $e^-/Å^3$ with an RMS deviation of 0.129 $e^-/Å^3$. On the basis of the final model, the calculated density was 1.916g/cm^3 and F(000), 1496 e^-.

Table S2. Sample and crystal data for Complex **1**.

Identification code	Complex 1	
Chemical formula	$C_{29}H_{27}F_3IrN_3O_4S$	
Formula weight	762.79 g/mol	
Temperature	100(2) K	
Wavelength	0.71073 Å	
Crystal size	0.142 x 0.203 x 0.302 mm	
Crystal habit	clear red Block	
Crystal system	monoclinic	
Space group	P 1 21/c 1	
Unit cell dimensions	a = 9.7042(13) Å	α = 90°
	b = 14.975(2) Å	β = 96.560(2)°
	c = 18.313(2) Å	γ = 90°
Volume	2643.8(6) $Å^3$	
Z	4	
Density (calculated)	1.916 g/cm^3	
Absorption coefficient	5.193 mm^{-1}	
F(000)	1496	

Table S3. Data collection and structure refinement for Complex **1**.

Diffractometer	Bruker APEX DUO	
Radiation source	fine-focus tube, MoKα	
Theta range for data collection	1.76 to 30.46°	
Index ranges	-13<=h<=13, -21<=k<=21, -26<=l<=26	
Reflections collected	65072	
Independent reflections	8003 [R(int) = 0.0723]	
Coverage of independent reflections	99.6%	
Absorption correction	multi-scan	
Max. and min. transmission	0.5260 and 0.3030	
Structure solution technique	direct methods	
Structure solution program	SHELXTL XT 2014/4 (Bruker AXS, 2014)	
Refinement method	Full-matrix least-squares on F^2	
Refinement program	SHELXTL XL 2014/7 (Bruker AXS, 2014)	
Function minimized	$\Sigma\, w(F_o^2 - F_c^2)^2$	
Data / restraints / parameters	8003 / 6 / 385	
Goodness-of-fit on F^2	1.038	
Δ/σ_{max}	0.002	
Final R indices	6740 data; I>2σ(I)	R1 = 0.0239, wR2 = 0.0481
	all data	R1 = 0.0329, wR2 = 0.0507
Weighting scheme	$w=1/[\sigma^2(F_o^2)+(0.0161P)^2+0.1290P]$ where $P=(F_o^2+2F_c^2)/3$	
Largest diff. peak and hole	0.729 and -0.635 eÅ^{-3}	
R.M.S. deviation from mean	0.129 eÅ^{-3}	

Crystal Structure Report for Complex ***12****.*

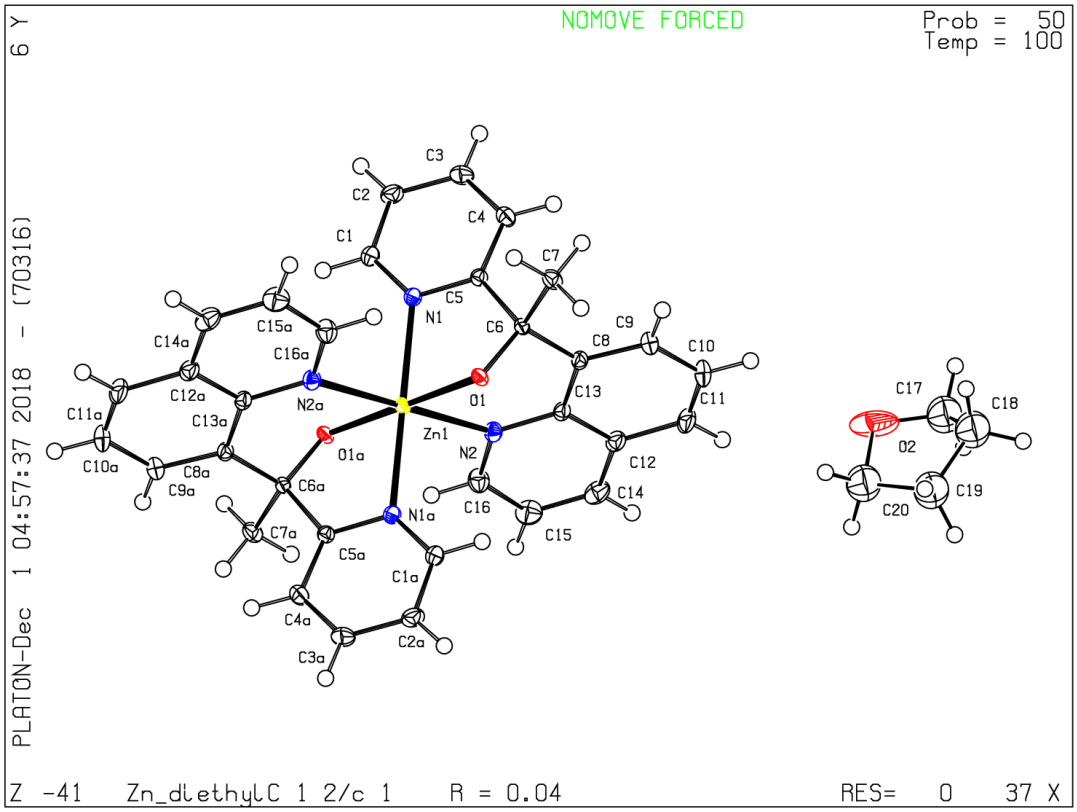

Figure S37. ORTEP diagram of **12**.

Description of Crystallography

A clear colorless blade-like specimen of $C_{32}H_{26}N_4O_2Zn$, approximate dimensions 0.080 mm x 0.130 mm x 0.320 mm, was used for the X-ray crystallographic analysis. The X-ray intensity data were measured on a Bruker APEX DUO system equipped with a TRIUMPH curved-crystal monochromator and a MoKα fine-focus tube (λ = 0.71073 Å).

A total of 2520 frames were collected. The total exposure time was 21.00 hours. The frames were integrated with the Bruker SAINT software package using a SAINT V8.37A (Bruker AXS, 2013) algorithm. The integration of the data using a monoclinic unit cell yielded a total of 35490 reflections to a maximum θ angle of 30.82° (0.69 Å resolution), of which 4522 were independent (average redundancy 7.848, completeness = 98.4%, R_{int} = 6.47%, R_{sig} = 4.25%) and 3487 (77.11%) were greater than $2\sigma(F^2)$. The final cell constants of a = 22.909(6) Å, b = 8.141(2) Å, c = 16.097(5) Å, β = 102.406(5)°, volume = 2932.0(14) $Å^3$, are based upon the refinement of the XYZ-centroids of reflections above 20 σ(I). Data were corrected for absorption effects using the multi-scan method (SADABS). The calculated minimum and maximum transmission coefficients (based on crystal size) are 0.7650 and 0.9330.

The structure was solved and refined using the Bruker SHELXTL Software Package, using the space group C 1 2/c 1, with Z = 4 for the formula unit, $C_{32}H_{26}N_4O_2Zn$. The final anisotropic full-matrix least-squares refinement on F^2 with 206 variables converged at R1 = 4.03%, for the observed data and wR2 = 9.87% for all data. The goodness-of-fit was 1.049. The largest peak in the final difference electron density synthesis was 0.892 $e^-/Å^3$ and the largest hole was -0.791 $e^-/Å^3$ with an RMS deviation of 0.086 $e^-/Å^3$. On the basis of the final model, the calculated density was 1.441g/cm^3 and F(000), 1328 e^-.

Table S4. Sample and crystal data for Complex **12**.

Identification code	Complex 12	
Chemical formula	$C_{32}H_{26}N_4O_2Zn$	
Formula weight	636.04 g/mol	
Temperature	100(2) K	
Wavelength	0.71073 Å	
Crystal size	0.080 x 0.130 x 0.320 mm	
Crystal habit	clear colourless blades	
Crystal system	monoclinic	
Space group	C 1 2/c 1	
Unit cell dimensions	a = 22.909(6) Å	α = 90°
	b = 8.141(2) Å	β = 102.406(5)°
	c = 16.097(5) Å	γ = 90°
Volume	2932.0(14) $Å^3$	
Z	4	
Density (calculated)	1.441 g/cm^3	
Absorption coefficient	0.883 mm^{-1}	
F(000)	1328	

Table S5. Data collection and structure refinement for Complex **12**.

Diffractometer	Bruker APEX DUO
Radiation source	fine-focus tube, MoKα
Theta range for data collection	1.82 to 30.82°
Index ranges	-31<=h<=32, -11<=k<=11, -23<=l<=22
Reflections collected	35490
Independent reflections	4522 [R(int) = 0.0647]
Absorption correction	multi-scan
Max. and min. transmission	0.9330 and 0.7650
Structure solution technique	direct methods
Structure solution program	SHELXTL XT 2014/5 (Bruker AXS, 2014)
Refinement method	Full-matrix least-squares on F^2
Refinement program	SHELXTL XL 2014/7 (Bruker AXS, 2014)
Function minimized	$\Sigma\, w(F_o^2 - F_c^2)^2$
Data / restraints / parameters	4522 / 7 / 206
Goodness-of-fit on F^2	1.049
Final R indices	3487 data; I>2σ(I) R1 = 0.0403, wR2 = 0.0903
	all data R1 = 0.0625, wR2 = 0.0987
Weighting scheme	$w=1/[\sigma^2(F_o^2)+(0.0425P)^2+4.9624P]$ where $P=(F_o^2+2F_c^2)/3$
Largest diff. peak and hole	0.892 and -0.791 eÅ^{-3}
R.M.S. deviation from mean	0.086 eÅ^{-3}

S7. References.

(1) Dreis, A. M.; Douglas, C. J. Catalytic Carbon-Carbon σ Bond Activation: An Intramolecular Carbo-Acylation Reaction with Acylquinolines. *J. Am. Chem. Soc.* **2009**, *131* (2), 412–413.

(2) van der Schaaf, P. A.; Wissing, E.; Boersma, J.; Smeets, W. J. J.; Spek, A. L.; van Koten, G. Organozinc Complexes with Monoanionic Chelating Phenolates or 2-Pyridylmethanolates. Molecular Structure of $[Zn(CH_2SiMe_3)\{OCH_2(2\text{-}Py)\}]_4$. *Organometallics* **1993**, *12* (9), 3624–3629.

(3) Prémont-Schwarz, M.; Barak, T.; Pines, D.; Nibbering, E. T. J.; Pines, E. Ultrafast Excited-State Proton-Transfer Reaction of 1-Naphthol-3,6- Disulfonate and Several 5-Substituted 1-Naphthol Derivatives. *J. Phys. Chem. B* **2013**, *117* (16), 4594–4603.

(4) Munitz, N.; Avital, Y.; Pines, D.; Nibbering, E. T. J.; Pines, E. Cation-Enhanced Deprotonation of Water by a Strong Photobase. *Isr. J. Chem.* **2009**, *49* (2), 261–272.

(5) Melhuish, W.H. Quantum Efficiencies of Fluorescence of Organic Substances: Effect of Solvent and Concentration of the Fluorescent Solute. *J. Phys. Chem.* **1961**, *65* (2), 229-235.